GastroPlus ver. 9.8.1 DDI Standards Update and Documentation Project

SimulationsPlus
SCIENCE + SOFTWARE = SUCCESS

Outline

- **Purpose:**

  This webinar will be an introduction to the GastroPlus DDI Standards Update project. This project is an extensive review of our current DDI Standards in order to update and document the input sources and assumptions for all of the substrates and perpetrators included in the GastroPlus (GP) library. This update will include addition of many new inhibition and induction mechanisms of perpetration for both enzymes and transporters. In addition to literature studies for current standards in the DDI Standards Update project, each one of the DDI standards will be accompanied by a full GP9.8.1 database, spreadsheet, slide set, and written report. The webinar will also provide a summary of the new mechanisms that have been added to midazolam, ketoconazole, gemfibrozil, and rifampicin.

  Methods:

  For each standard, the GP9.8.1 database has been extensively documented with literature references and if any parameters are fitted, that is described in the comments section. An Excel spreadsheet will be prepared, listing physicochemical, biochemical, and biopharmaceutical properties and sources of information. Also, *in vivo* preclinical (if any), and clinical studies used in development of the PBPK models and in the validation of each mechanism of DDI will be included. An MS-PowerPoint document will summarize the model development for each standard and finally an MS-Word report (suitable for inclusion in regulatory submissions) will be prepared.

  Results:

  Updates and documentation have been completed or will soon be released for 3A4 substrates midazolam, triazolam, and alfentanil and 2C8 substrates repaglinide and rosiglitazone. Also available for download will be the following perpetrators: fluconazole (validated for moderate reversible 3A4 inhibition), ketoconazole (validated for strong 3A4 rev. and irrev. inhibition), voriconazole (validated for strong rev. and irrev. 3A4 inhibition), and rifampicin (validated for strong induction of 3A4, 2C8, and 2C9). Many other DDI mechanisms are included in the perpetrator tables and additional validation documentation will be released as it becomes available from the DDI Task Force. In addition, you will see a new column in the Perpetrator Table that highlights which entries have been validated.

  Conclusions:

  This DDI Update project will be an extensive and time-consuming process. In the next few years, Simulations Plus will update the databases and documentation for more than 40 DDI substrates and perpetrators. These resources will be available for licensed users to download.

Primary Focus

- This webinar will describe or provide:
  - How to approach and document any project involving mechanistic absorption and PBPK simulations.
  - Description of the historical GastroPlus (GP) database of substrate and perpetrator DDI standards and a discussion of how these standards are being extensively documented for the development and validation of simulation models.
  - A process of DDI Standard development and documentation that is currently available to users who request the information.
- This webinar is not:

However, the next couple of slides will help answer those questions.

DDI Module –PBPK Models in various stages of validation: Probe Substrates, Inhibitors, and Inducers

Alfentanil	Dolutegravir	Metformin	Rifampicin	Warfarin
Atazanavir	Efavirenz	Midazolam	Rivaroxaban	
Atomoxetine	Fexofenadine	Omeprazole & Metab.	Rosiglitazone	
Buproprion	Fluconazole	Phenytoin	Rosuvastatin	
Caffeine	Fluvoxamine	Posaconazole	Theophylline	Atorvastatin
Cyclosporine	Gemfibrozil & glucuronide	Pravastatin	Tolbutamide	Simvastatin
Desipramine	Imipramine	Quinidine	Triazolam	
Digoxin	Itraconazole &Metab.	Raltegravir & Metab.	Verapamil	
Diltiazem & Metab.	Ketoconazole	Repaglinide	Voriconazole	

Progress – Initial DDI Standard Updates Addressed: Probe Substrates, Inhibitors, and Inducers

Efavirenz, Fluconazole, Gemfibrozil and glucuronide, Ketoconazole, Itraconazole + 3 metabolites, Midazolam, Repaglinide, Rifampicin, Voriconazole, Rosiglitazone, Triazolam

- Literature collection complete and collated in spreadsheet
- Model building and validation of single compound
- Validation for all mechanisms of DDI
- PowerPoint
- MS-Word Reports

As we are prioritizing the next batch of DDI standards to build and/or update, we welcome your feedback on compounds that are most important for your projects.

Outline of Process for Model Development and Documentation

- Creation of GP a project starts with structure import using ADMET Predictor Module for both substrates and perpetrators.
  - Physicochemical, biopharmaceutical, and biochemical properties
  - Initial evaluation via “Chemistry Classification” with all aspects of ADMET
    - Solubility vs. pH, dissolution, absorption (w/ influx and efflux transporters), clearance (metabolic, biliary, and renal), distribution, excretion, and toxicity.
  - Extensive literature collection and spreadsheet documentation.
    - Workbook with multiple sheets for Physicochemical, Metabolic, Transporter, Preclinical, and Clinical single compound and DDI study data for multiple perpetration mechanisms.
  - First simulations for “Measured Properties” with parameter sensitivity analysis.
  - Model building for individual substrate and/or perpetrator simulations compared to observed data for single escalating doses (for nonlinear dose dependence), multiple dosing (for autoinhibition / autoinduction).
  - DDI simulations for all appropriate mechanisms on both substrate and perpetrator.
  - Analysis of results using the “Guest”* criterion for different levels of accuracy cutoff for increasing AUC (inhibition) and decreasing AUC (induction).
  - Preparation of slides and written reports suitable for regulatory submission.

Gemfibrozil BCS II Physicochemical Properties

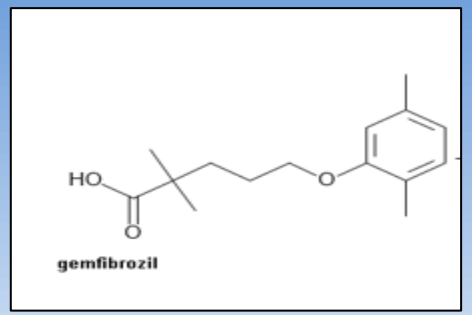

MW = 250.34

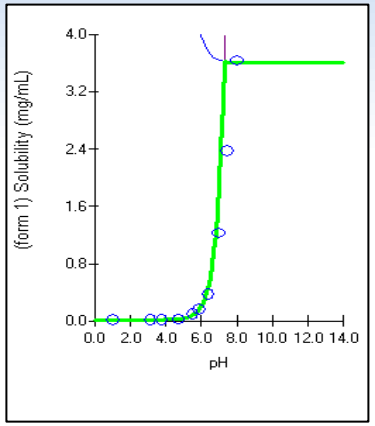

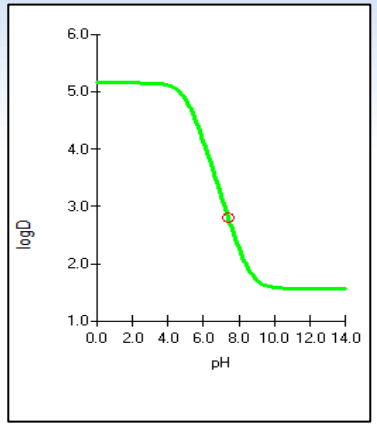

Estimated Solubility Factor after fitting pH Vs solubility profile = 156.9
Adjusted Sol factor = 180

AP 10.0 = ADMET Predictor v. 10.0
S+ = properties predicted with Simulations Plus models
S+Sw = native solubility in pure water
S+Peff = human jejunal permeability estimate
N.A = Not Available

S+LogP = 4 (AP 10.0)
Exp LogD (Octanol/H2O) @ pH7.4 = 2.8 (Luner et. al., Pharm. Res.11(12):1755 (1994)
NOTE: Changed LogD (7.4) = 0.8 to calculate Kps then changed back to 2.8 to run simulations.

S+pKa = 4.92 (Acid) (AP 10.0
Exp pKa = 5 (Luner et. al., Pharm. Res.11(12):1755 (1994)

S+Sw = 0.0826 mg/ml @ pH 4.24 (AP 10.0)
Exp Sw = 0.02 mg/ml @ pH 1 37 deg C (LOW) (Luner et. al., Pharm. Res.11(12):1755 (1994)
S+Solubility Factor = 276.89
S+FaSSIF = 0.42 mg/ml, S+ FeSSIF = 0.62 mg/ml (AP 10.0)
Exp FaSSIF = N.A

S+Peff = 7.33x 10^{-4} (cm/s) (AP 10.0) (HIGH)
Caco-2 Papp A->B = 5.89E-5 (Absorptions Systems Lighthouse Database)
Caco-2 Papp B->A = 4.73E-5 (Absorptions Systems Lighthouse Database)
Caco-2 Converted to Hum Peff = 5.60E-4 cm/s (From GeoMean =5.28E-5 cm/s from Abs Sys Caco-2)

S+hum_fup% = 5.18 %(AP 10.0)
Exp. Fup = 3.5%(Oprea and Benet Wombat database)
S+RBP = 0.67(AP 10.0)
Exp Rbp =0.75(Deguchi et. al., Drug.Metab.Dispos.39(5):820 (2011)

S+Enzyme Substrate: CYP2C9(48%), CYP2C19(71%), UGT1A1(68%), UGT1A3(97%), UGT1A9(76%), UGT2B7(93%)
S+Transporter Substrate: P-gp(75%), OATP1B1(99%), OAT1(87%),
Exp Enzyme Substrate: 2C9, 2C19, UGT1A3, UGT2B7
Exp Transporter Substrate: OATP1B1 (liver influx)

S+Enzyme Inhibitor: CYP2C9(77%)
S+Transporter Inhibitor: OAT1(95%), OAT3(76%),
Exp Enzyme Inhibitor: 2C8, 2C9
Exp Transporter Inhibitor: NTCP, OAT3, OATP1B1, OATP1B3

Gemfibrozil AP10.0 Transporter Classification

- Transporter Substrate Classification:
  - **OATP1B1-Substrate=Yes (99%);** OATP1B3-Substrate=No (60%); **OCT1-Substrate=Yes (96%); OCT2-Substrate=Yes (74%); OAT1-Substrate=Yes (87%)**; **OAT3-Substrate=Yes (75%)**; **Pgp-Substrate=Yes (75%);** BCRP-Substrate=No (95%);
- Transporter Km Values:
  - OATP1B1-Km=24.62uM; OATP1B3-Km=66.47uM; OCT1-Km=8.66uM; OCT2-Km=18.12uM; OAT1-Km=25.48uM; OAT3-Km=122.11uM;
- Transporter Inhibitor Classification:
  - OATP1B1-Inhibitor=No (54%); OATP1B3-Inhibitor=No (96%); OCT1-Inhibitor=No (77%); OCT2-Inhibitor=No (99%); **OAT1-Inhibitor=Yes (95%); OAT3-Inhibitor=Yes (76%);** Pgp-Inhibitor=No (96%); BSEP-Inhibitor=No (66%); BCRP-Inhibitor=No (97%);
- Transporter IC50 Values:
  - BSEP-IC50=48.26uM;

pH-solubility *in vitro* data of Gemfibrozil

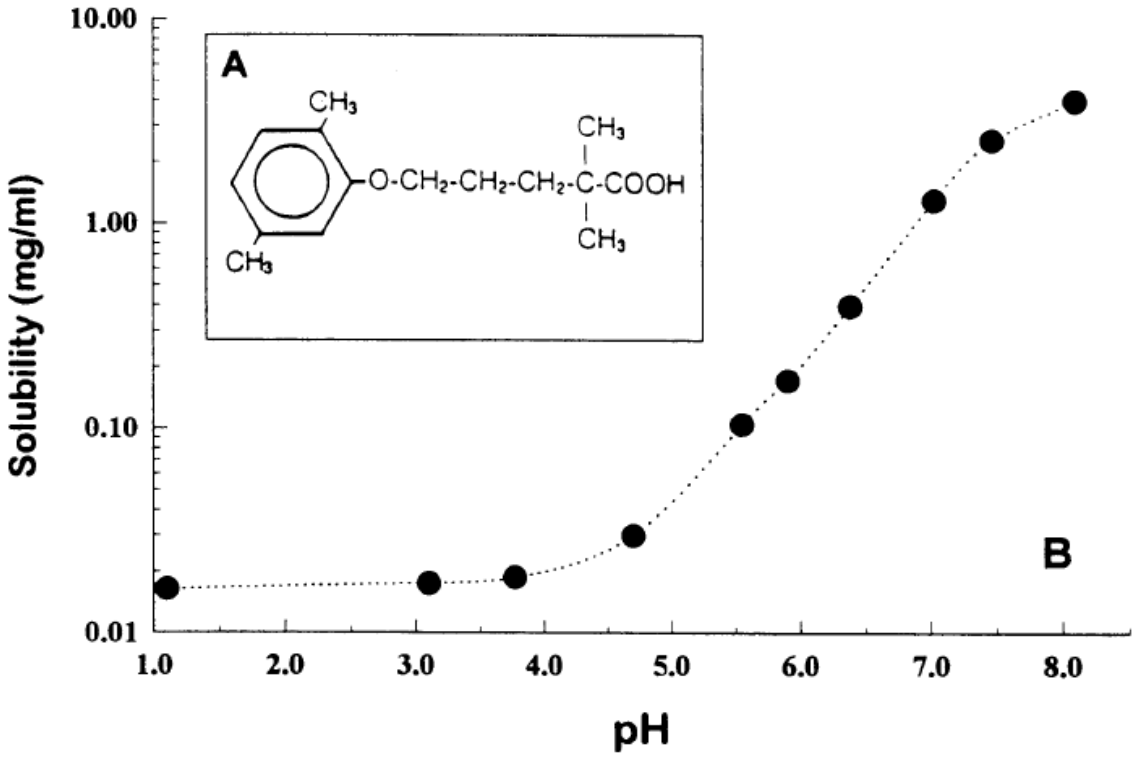

Fig. 1. (A) Chemical structure of gemfibrozil (5-(2,5-dimethyl-phenoxy)-2,2-dimethylpentanoic acid). The molecular weight is 250.4 (B) Gemfibrozil pH-solubility profile, 37°C. Each data point represents the mean (n = 3) and SD is within the symbols.

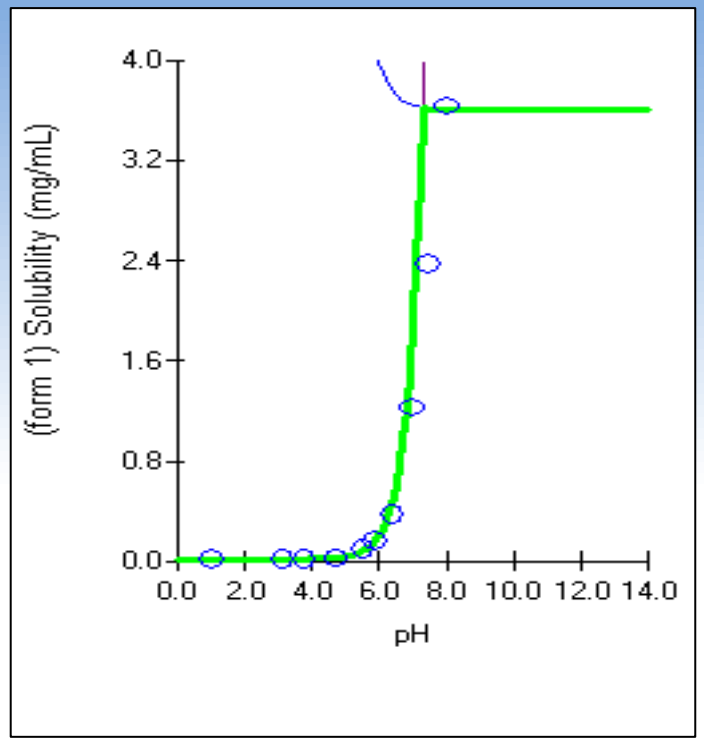

After fitting the pH-solubility profile
Acid pKa =5.025
Sol factor= 180

Luner et al., Pharm. Res. 11(12):1755 (1994)

Gemfibrozil Glucuronide Physicochemical Properties

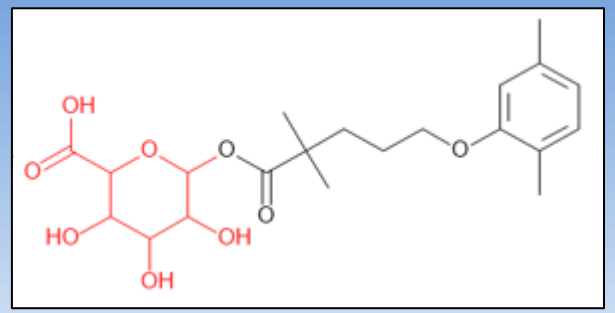

MW = 426.47

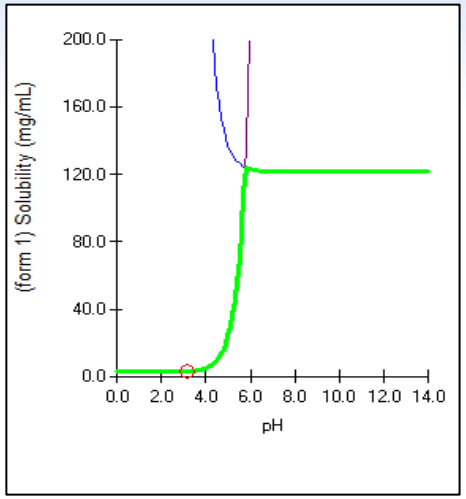

AP 10.0 = ADMET Predictor v. 10.0
S+ = properties predicted with Simulations Plus models
S+Sw = native solubility in pure water
S+Peff = human jejunal permeability estimate
N.A = Not Available

S+LogP = 1.67(AP 10.0)
Exp LogD (Octanol/H2O) @ pH7.4
Exp log P extrapolated from Log D

S+pKa = 4.12 (Acid)
Exp pKa = N.A

S+Sw = 3.0900 mg/ml @ pH 3.15 (AP 9.5)
Exp Sw =N.A
S+Solubility Factor = 43.48
S+FaSSIF = 1.13 mg/ml, S+ FeSSIF = 2.71 mg/ml
Exp FaSSIF =N.A

S+Peff = 4.0E-5 (cm/s) (AP 10.0)

S+hum_fup% = 11.2% (AP 10.0)
Exp. Fup% =11.5% (Shitara et al., J.Pharmacol. Exp.Ther. 311(1):228(2004)
NOTE: For all simulations Fup% = 5.0 to correct the Vdss for glucuronide

S+RBP = 0.65 (AP 10.0)
Exp Rbp =N.A

S+Enzyme Substrate:
Exp Enzyme Substrate: Hydrolase
S+Transporter Substrate: P-gp(99%), OATP1B1(99%), OATP1B3(93%), OAT1(65%), OAT3(97%), OCT1(76%)
Exp Transporter Substrate: OATP1B1 (liver influx), OAT3 (kidney influx), MRP2 (liver-bile efflux), MRP3 (liver-systemic efflux), MRP4 (kidney-tubule efflux)

S+Enzyme Inhibitor: CYP2C9(35%), CYP3A4(42%)
S+Transporter Inhibitor:
Exp Enzyme Inhibitor: 2C8, 2C9
Exp Transporter Inhibitor: NTCP, OAT3, OATP1B1, OATP1B3

Gemfibrozil Glucuronide AP10.0 Transporter Classification

- Transporter Substrate Classification:
  - OATP1B1-Substrate=Yes (99%); OATP1B3-Substrate=Yes (92%); OCT1-Substrate=Yes (76%); OCT2-Substrate=No (91%); OAT1-Substrate=Yes (65%); OAT3-Substrate=Yes (97%); Pgp-Substrate=Yes (99%); BCRP-Substrate=No (95%);
- Transporter Km Values:
  - OATP1B1-Km=42.7uM; OATP1B3-Km=74.53uM; OCT1-Km=6.99uM; OCT2-Km=2.99uM; OAT1-Km=24.36uM; OAT3-Km=50.64uM;
- Transporter Inhibitor Classification:
  - OATP1B1-Inhibitor=No (54%); OATP1B3-Inhibitor=No (49%); OCT1-Inhibitor=No (89%); OCT2-Inhibitor=No (99%); OAT1-Inhibitor=No (94%); OAT3-Inhibitor=No (83%); Pgp-Inhibitor=No (96%); BSEP-Inhibitor=No (99%); BCRP-Inhibitor=No (97%);
- Transporter IC50 Values:
  - BSEP-IC50=41.79uM;

Extended Clearance CS (ECCS)

Compound are assigned to one of six classes based on:

1) High or low permeability
2) High or low MW (400 g/mol)
3) Ionization class: Acids/Zwitterions versus Bases/Neutrals

Class 1A and 2 are metabolism
Classes 3A and 4 are renal
Class 1B is hepatic uptake
Class 3B is hepatic uptake or renal

Varma M., et. al. Pharm. Res. 2015, 32, 3785.

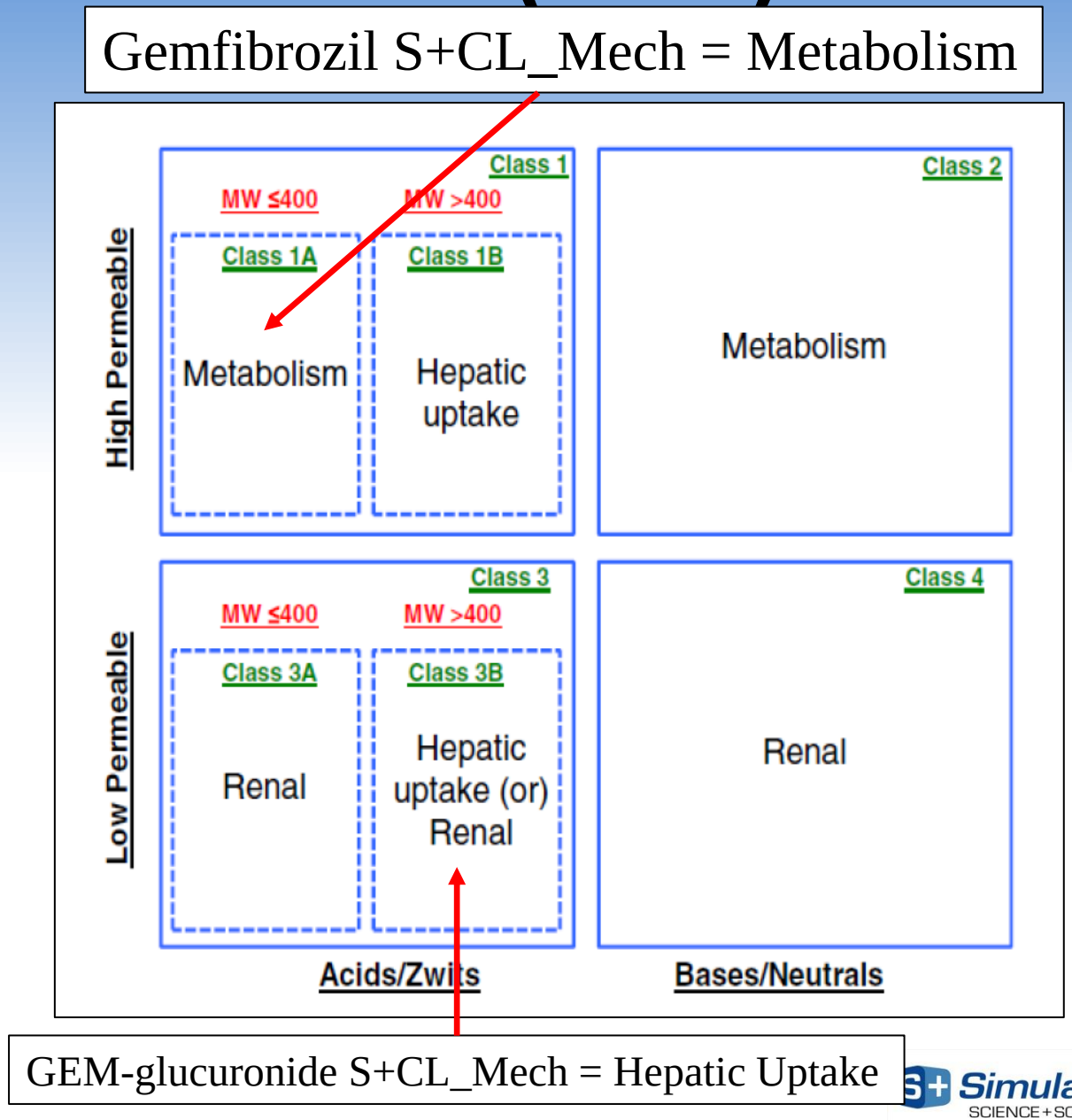

Varma and ADMET Predictor ECCS models

Varma ECCS

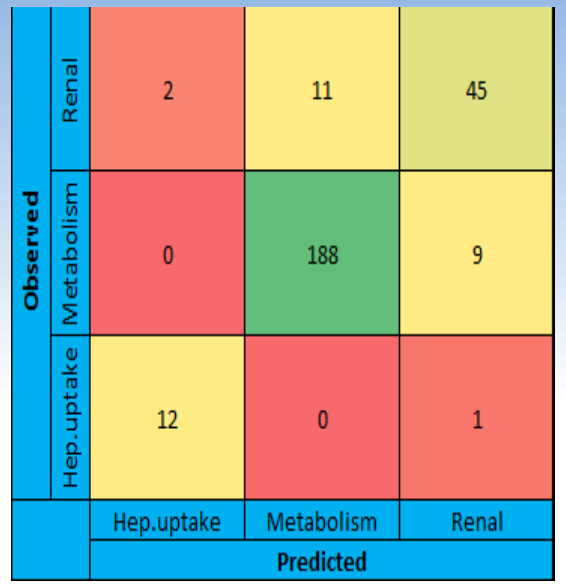

S+Hum CL Mech.

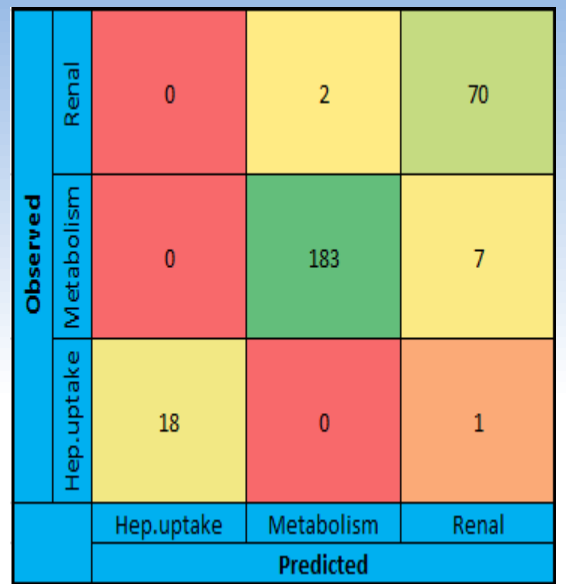

Statistic	ECCS	Hum CL Mech Bin
Concordance	91%	96%
Youden	0.78	0.94
Coverage	88%	92%

Varma M., et. al. Pharm. Res. 2015, 32, 3785.

Purely *in silico* model

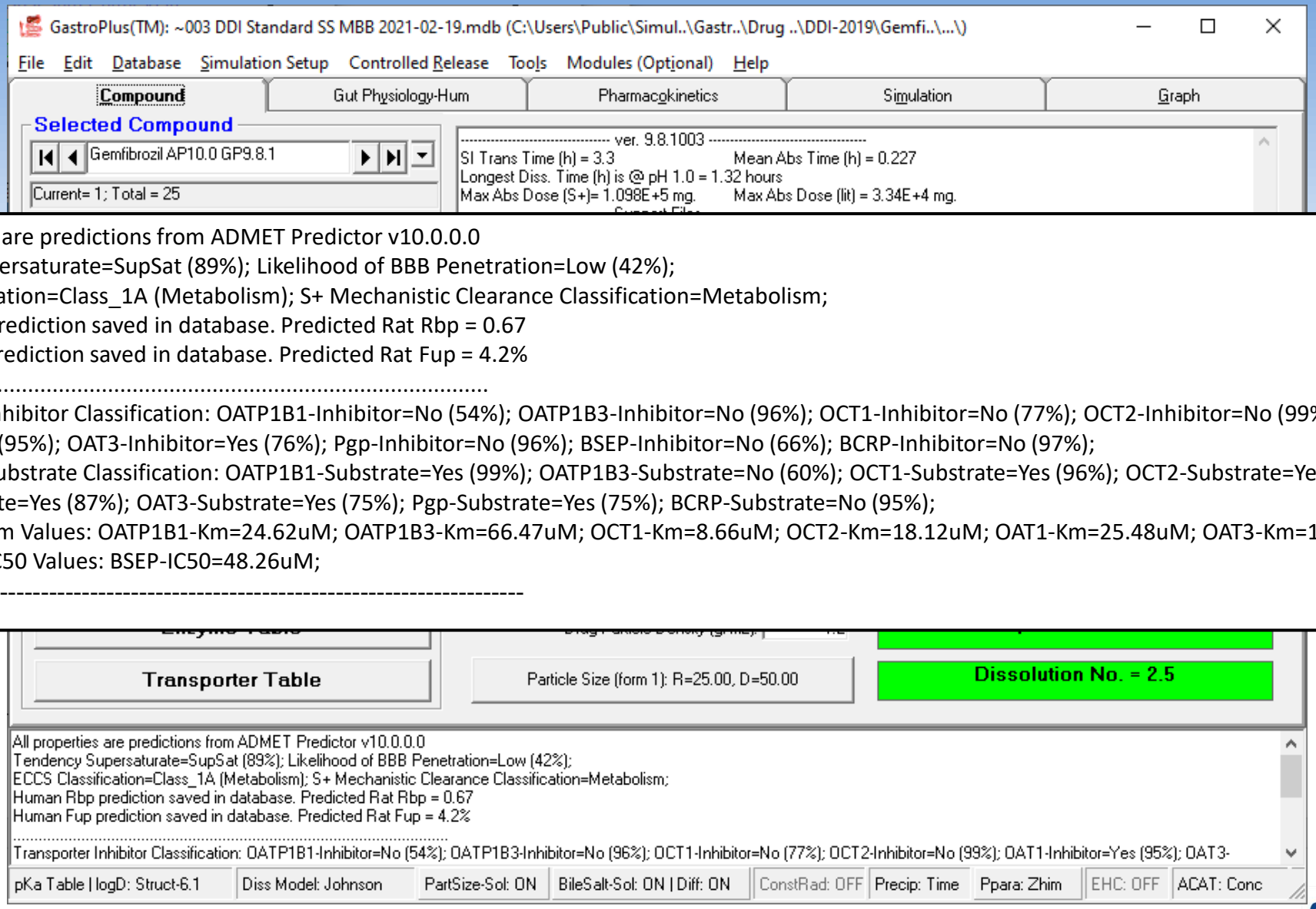

SimulationsPlus
SCIENCE + SOFTWARE = SUCCESS

Hum PO 900 mg Tab *in silico vs.* Honkalammi

Purely *in silico*

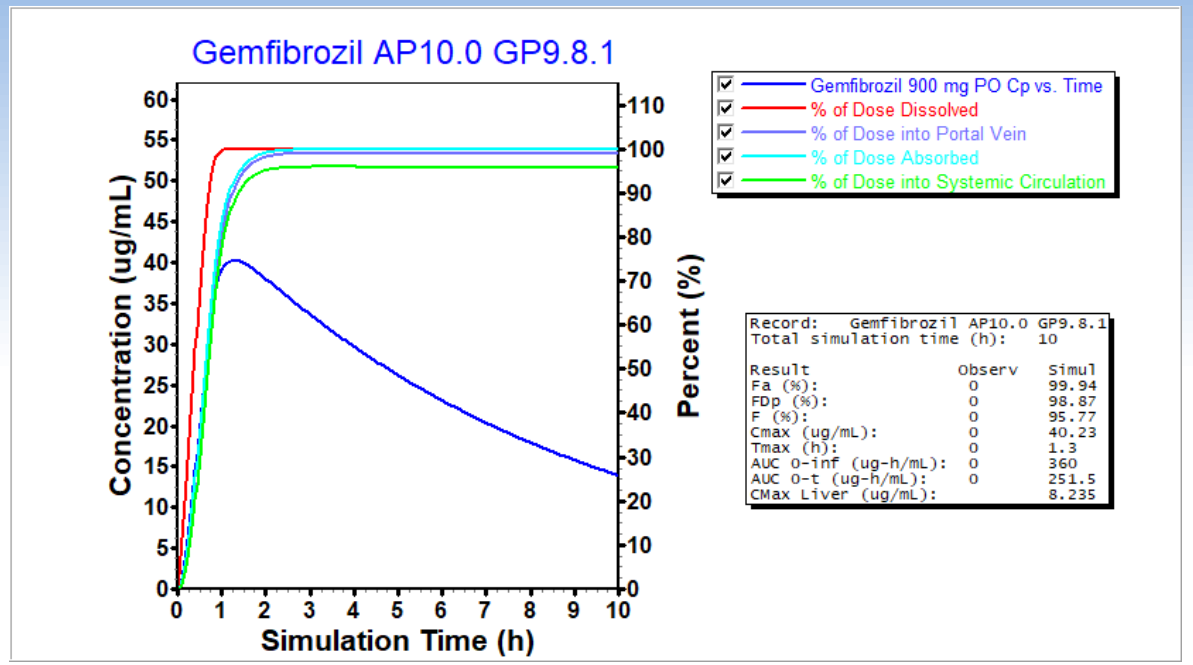

All mechanisms *in silico, in vitro, & fitted*

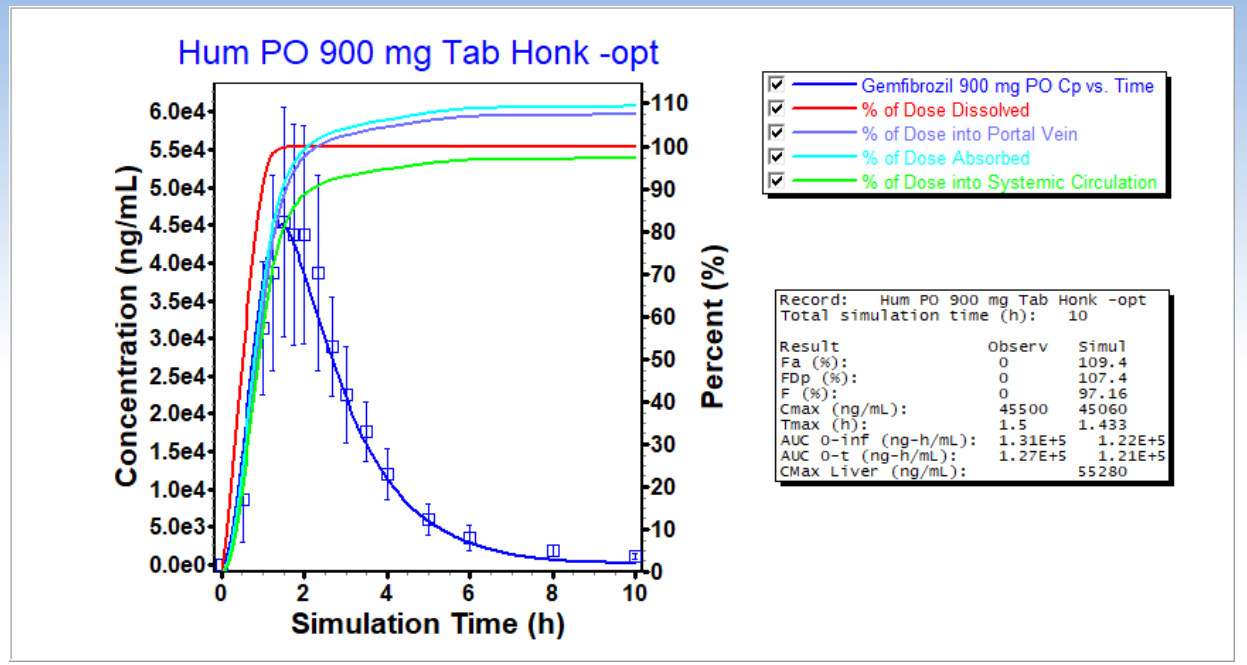

Physiology used: Healthy Male 23 years 73 Kg 23 BMI

All mechanisms PBPK Model: Liver and Kidney were assumed Permeability limited organs; the rest were assumed perfusion limited Kps for the Glucuronide record were calculated using the Poulin-extracellular method was used for both Perfusion Limited and for Permeability limited tissues.

Honkalammi et.al., Drug. Metab. Dispos. 39(10):1977(2011)

Conclusions and Recommended Testing Based on *in silico* properties

- Low solubility in stomach probably won't reduce bioavailability but may result in slow dissolution and longer T_{max}.
- Low MWt, high permeability, and acidic pKa of parent GEM suggest mainly metabolic clearance by Phase I (2C9 and 2C19) and Phase II (UGT1A3 and UGT2B7) enzymes.
- AP10.0 transporter module suggests possible liver and kidney influx.
- High MWt, low permability, and acidic pKa of GEM-glucuronide suggests systemic clearance by hepatic and renal influx.
- Both parent and glucuronide metabolite may be involved in DDI inhibition of enzymes.

Outline of Process for Model Development and Documentation

- Creation of GP a project starts with structure import using ADMET Predictor Module for both substrates and perpetrators.
  - Physicochemical, biopharmaceutical, and biochemical properties
  - Initial evaluation via “Chemistry Classification” with all aspects of ADMET
    - Solubility vs. pH, dissolution, absorption (w/ influx and efflux transporters), clearance (metabolic, biliary, and renal), distribution, excretion, and toxicity.
  - Extensive literature collection and spreadsheet documentation.
    - Workbook with multiple sheets for Physicochemical, Metabolic, Transporter, Preclinical, and Clinical single compound and DDI study data for multiple perpetration mechanisms.
  - First simulations for “Measured Properties” with parameter sensitivity analysis.
  - Model building for individual substrate and/or perpetrator simulations compared to observed data for single escalating doses (for nonlinear dose dependence), multiple dosing (for autoinhibition / autoinduction).
  - DDI simulations for all appropriate mechanisms on both substrate and perpetrator.
  - Analysis of results using the “Guest”* criterion for different levels of accuracy cutoff for increasing AUC (inhibition) and decreasing AUC (induction).
  - Preparation of slides and written reports suitable for regulatory submission.

Human Cp vs. time profiles before and after GEM and GEM-glucuronide DDIs

Subset of 13 references from a total of 83:

1. Hermening-JChromatogrBBiomedSci-741-2-129-2000-PK profiles-of-gemfibrozil-and-glucuronide-and-covalent-adducts-PO-900-mg
2. Hirano-DrugMetabDisp-34-7-1229-2006-DDI-Pitavastatin-Verapamil-Ki-hepatic-uptake-OAT1B1
3. Ho-Gastroenterology-130-6-1793-2006-Rosuvatatin-hepatic-uptake-OATP and NTCP-Vmax-Km transporters
4. Honkalammi-DrugMetabDispos-39-10-1977-2011-Human data-Repaglinide-Gemfibrozile DDI-2C8 activity
5. Kajosaari-Backmann-BasicClinPharmcolToxicol-97-249-2005-Metabolism-Repaglinide-Gemfibrozil-CYP2C8-Ki-CYP3A4
6. Nakagomi-Xenobiotica-37-4-416-2007_Inhibition of hOAT3 pravastatin transport by gemfibrozil and glucuronide human
7. Nakagomi-Hagihara-Xenobiotica-37-5-474-2007-Gemfibrozil-and-its-glucuronide-inhibit-OATP1B1
8. Ogilvie-DrugMetabDispos-34-1-191-2006-Gemfibrozil Glucuronide-HLM study-NADPH dependent inactivation-2C8
9. Schneck-ClinPharmacolTher-75-5-455-2004-Rosuvastatin and Gemfibrozil DDI
10. Wang-CPT- PharmacometSysPharmacol-6-4-228-2017-Transporter Based DDI Rosuvastatin PBPK model SimCyp
11. Wen-Neuvoven-DrugMetabDisposition-29-11-1359-2001-invitro-2C9 inhibition-Gemfibrozil
12. Yamazaki-Lin-Xenobiotica-35-7-737-2005-OATP1B1-MRP2-P-gp-mediated transport-Gemfibrozil-DDI-Fibric acid derivatives
13. Yoshida-ClinPharmTherap-91-6-1053-2012-Transporter-DDI-of-OATP-Substrates-from-in-vitro-studies-w-Supplements

Extensive Workbook for all DDI Standards

	A	B	C	D	E
1	Gemfibrozil Physicochemical Properties			MWt	
2	SS, 05\18\2020 Updated 09\22\2020			250.34	
3					
4					
5		**Property**	**Value**	**Units**	**Ref.**
6		S+logP	4		ADMET Predictor ver. 10.0
7		Exp log D (Oct/H2O)@pH 7.4	2.8		Luner-Radebaugh-PharmRes-11-12-1755-1994-Gemfibrozil-pH sol
8		Exp log P extrapolated from Log D	5.2		GP 9.7
9		**pKas**			
10		S+Acid pKa	4.92		ADMET Predictor ver. 10.0
11		Exp Acid pKa	5		Luner-Radebaugh-PharmRes-11-12-1755-1994-Gemfibrozil-pH sol
12		**Solubility**			
13		S+Sw	0.0826	mg/mL	ADMET Predictor ver. 10.0
14		S+pH	4.24		ADMET Predictor ver. 10.0
15		S+Solublity Factor	276.89		ADMET Predictor ver. 10.0
16		Aq. Sol from GSE	0.00213	mg/mL	Yalkowsky GSE
17		Exp. Solubility @ pH 1 @37 deg C	0.02000	mg/mL	Luner-Radebaugh-PharmRes-11-12-1755-1994-Gemfibrozil-pH sol
18		S+FaSSIF @ pH 6.5	0.4200	mg/mL	ADMET Predictor ver. 10.0
19		S+FeSSIF @ pH 5.0	0.6200	mg/mL	ADMET Predictor ver. 10.0
20		**Permeability**			
21		S+Peff	7.33E+04	cm/s	ADMET Predictor ver. 10.0
22		Caco-2 Papp A->B	5.89E-05		Absorptions Systems Lighthouse Database
23		Caco-2 Papp B->A	4.73E-05		Absorptions Systems Lighthouse Database
24		Ratio B->A / A->B	0.80		
25		GeoMean B->A and A->B	5.28E-05		Absorptions Systems Lighthouse Database
26		P-gp Substrate	No	Yes/No	
27		Caco-2 Converted to Hum Peff	5.60E-04	cm/s	Converted from GeoMean of Absorption Systems Caco-2
28		**Blood to Plasma Conc. Ratio**			
29		S+Rbp	0.67		ADMET Predictor ver. 10.0
30		Ex Rbp			
31		Fitted for PBPK			
32		**Fraction Unbound in Plasma**			
33		S+PrUnbnd	5.18	%	ADMET Predictor ver. 10.0
34		Ex fup	3.5	%	Oprea and Benet Wombat database
35		Ex fup	2	%	Miller-ClinPharmacokinet-34-2-155-1998-Clinical PK of Fibric Acid
36		**Melting Point**			

Gemfibrozil-Physicochemical | GGluc-Physicochemical | Metabolism-Hermening 2000 | Metab & CLint-UGT | Transporter-OATP1B1 | CYP E

Estimated free base solubility using GSE Ref. Sanghvi-Yalkowsky-QSARCombSci-22-2-258-2003-Estima

log S = 0.5 – 0.01(m.p. °C – 25) – log P solution logS= 0.5 -0.01(122-25)-3.97= -4.45

Aq. Sol

-5.07E+00 Log Sol (M)

8.51E-06 **M**

0.002 g/L

ISIS/Base

File Edit Options Object Database Search List Window Help

BIOBYTEMASTER-2008.DB/Main

ISIS/Base

File Edit Options Object Database Search List Window Help

ABS-SYSTEMS-LIGHTHOUSE-DATABASE-MBB-3-15-05.DB/Main

Forms | Query | Browse | Update

<Root> Search Domain: All 1 of 1

Structure	ID	LDS_PN
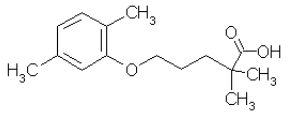	186	L0186
	Compound_Name: Gemfibrozil	CAS_RegistryNumber: 25812-30-0
	*fmla_Structure: $C_{15}H_{22}O_3$	*mol.weight_Structure: 250.3408
	Selected	Therapeutic_Category: Antihyperlipoproteinemic

PctBound_HumanPlasmaProt_Log	PctBound_RatPlasmaProt_Log	OralBioavailability_LitValue	MolWeight_LDS_File
		98.0000	250.3000
PctRemaining_HumanLiverMsomes	PctRemaining_RatLiverMsomes	Papp_Caco2_AB_Log (Papp x 10E6)	Papp_Caco2_BA_Log
35.3000	67.5000	1.7699	1.6746
BrainPlasmaRatioRat_Log	Clearance_LitValue (L/h)	Papp_MDR_MDCK_AB_Log	Papp_MDR_MDCK_BA_Log
	1.7000		
DoseNumber_LitValue	EffluxRatio_Caco2_Log	pKa1	pKa2
240.0000	-0.0953	4.8900	
EffluxRatio_MDR_MDCK_Log	HIA_LitValue	pKa3	HIA_LitValue
InVitroHalfLife_HumanLvrMsomes (min)	InVitroHalfLife_RatLiverMsomes (min)	Solubility_LitValue (mg/mL)	Solubility_pH20 (mg/mL)
63.3000	37.9000	0.0100	
LogP_Predicted	LogP	Solubility_pH74	Uptake_RatBrainPerfusion_Log
4.8000	4.6370		
MaximumDoseStrength_LitValue	VolumeOfDistribution_LitValue (L/Kg)	CLint_uL_min_milCells	CLint_mL_min_mg
0.0100	0.1400		
Papp_Caco2_AB_BCS_pH65	Recov_Caco2_AB_BCS_pH65	Papp_Caco2_AB_BCS_pH74	Recov_Caco2_AB_BCS_pH74

Extensive Workbook for all DDI Standards

A1 | Gemfibrozil and Gem Glucuronide inhibits uptake of pravastatin mediated by OATP1B1

Gemfibrozil and Gem Glucuronide inhibits uptake of pravastatin mediated by OATP1B1
Ref: Nakagomi-hagihara-Xenobiotica-37-5-474-2007-Gemfibrozil-and-its-glucuronide-inh-OATP1B1
SS, 06/15/2020

Abstract

When pravastatin (40 mg/day) was co-administered with gemfibrozil (600 mg, b.i.d., 3 days) to man, the AUC of pravastatin increased approximately 2-fold. We have clarified that OATP1B1 is a key determinant of the hepatic uptake of pravastatin in humans. Thus, we hypothesized that gemfibrozil and the main plasma metabolites, a glucuronide (gem-glu) and a carboxylic acid metabolite (gem-M3), might inhibit the hepatic uptake of pravastatin and lead to the elevation of the plasma concentration of pravastatin. Gemfibrozil and gem-glu inhibited the uptake of ^{14}C-pravastatin by human hepatocytes with K_i values of 31.7 μM and 15.7 μM, respectively and also inhibited pravastatin uptake by OATP1B1-expressing Xenopus laevis oocytes with K_i values of 15.1 μM and 7.6 μM. Additionally, we examined the biliary transport of pravastatin and demonstrated that pravastatin was transported by MRP2 using both human canalicular membrane vesicles (hCMVs) and human MRP2-expressing vesicles. However, gemfibrozil, gem-glu and gem-M3 did not affect the biliary transport of pravastatin by MRP2. Considering the plasma concentrations of gemfibrozil and gem-glu in humans, the inhibition of OATP1B1-mediated hepatic uptake of pravastatin by gem-glu would contribute, at least in part, to the elevation of plasma concentration of pravastatin by the concomitant use of gemfibrozil.

Ref: Nakagomi-hagihara-Xenobiotica-37-5-474-2007-Gemfibrozil-and-its-glucuronide-inh-OATP1B1 Gemfibrozil and its Glucuronide mediated inhibition of Uptake of Pravastatin via OATP1B1							
OATP1B1 inhibition by Gemfibrozil in OATP1B1 expressing Xenopus Laevis oocytes							
Ki (Gemfibrozil)	15.1	μM					
Concentration of Gemfibrozil	20	μM					
OATP1B1 inhibition by Gemfibrozil Glucuronide in OATP1B1 expressing Xenopus Laevis oocytes							
Ki (Gem Gluc)	7.6	μM					
Concentration of Gemfibrozil Glucuro	20	μM					

OATP1B1 inhibition by Gemfibrozil using cryopreserved Hepatocytes						
Ki (Gemfibrozil)	31.7	μM				
Concentration of Gemfibrozil	20	μM				
OATP1B1 inhibition by Gemfibrozil Glucuronide in OATP1B1 cryopreserved Hepatocytes						
Ki (Gem Gluc)	15.7	μM				
Concentration of Gemfibrozil Gluc	20	μM				

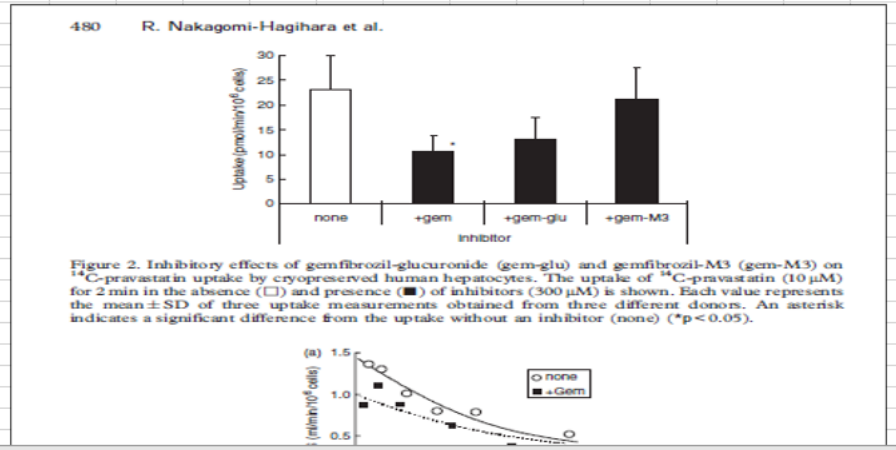

Figure 2. Inhibitory effects of gemfibrozil-glucuronide (gem-glu) and gemfibrozil-M3 (gem-M3) on ^{14}C-pravastatin uptake by cryopreserved human hepatocytes. The uptake of ^{14}C-pravastatin (10 μM) for 2 min in the absence (□) and presence (■) of inhibitors (300 μM) is shown. Each value represents the mean ± SD of three uptake measurements obtained from three different donors. An asterisk indicates a significant difference from the uptake without an inhibitor (none) (*$p < 0.05$).

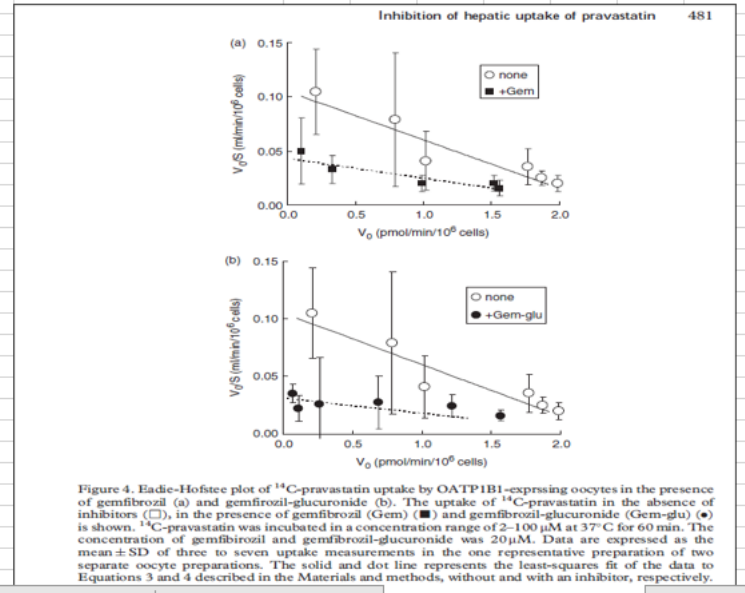

Figure 4. Eadie-Hofstee plot of ^{14}C-pravastatin uptake by OATP1B1-exprssing oocytes in the presence of gemfibrozil (a) and gemfirozil-glucuronide (b). The uptake of ^{14}C-pravastatin in the absence of inhibitors (□), in the presence of gemfibrozil (Gem) (■) and gemfibrozil-glucuronide (Gem-glu) (●) is shown. ^{14}C-pravastatin was incubated in a concentration range of 2–100 μM at 37°C for 60 min. The concentration of gemfibrozil and gemfibrozil-glucuronide was 20 μM. Data are expressed as the mean ± SD of three to seven uptake measurements in the one representative preparation of two separate oocyte preparations. The solid and dot line represents the least-squares fit of the data to Equations 3 and 4 described in the Materials and methods, without and with an inhibitor, respectively.

Transporter-OATP1B1 | CYP Enzymes-Invitro Inhibition | CYP2C8-invitro inhibition | Transporter-OATP1B1 Inhibition | Transp-OATP inhibition | Transp-OATP1B1-Nakagomi | Transp-OATP1I ...

SimulationsPlus
SCIENCE + SOFTWARE = SUCCESS

Extensive Workbook for all DDI Standards

All subjects received 3 mg oral MDZ, followed by the indicated dose of oral ALF. Results are given as mean ± SD (N = 10).
ND, Not determined (the calculated F_G for MDZ after rifampin was either zero or indefinite because F_H was zero); CL/F, oral clearance; V_c/F, volume of central compartment; F_{oral}, oral bioavailability; F_G, intestinal bioavailability; CL_{mucosa}, effect clearance.
*Significantly different from same-dose control ($P < .05$).

GastroPlus(TM) 9.8.0008	12/23/2020	9:24:33 AM						
Compound 1:	Victim							
Database:	Midazolam-GP-9.7-DDI-Standard-VL-2020-09-07-MBB-2020-12-22.mdb							
Record:	Midaz PO 3.0mg vs RIF 600mg 5d Kharasch							
Compound 2:	**Perpetrator: 3A4 ind. & inh., UGT1A3 ind., MRP2 inh., and OATP1B1 inh.**							
Database:	Rifampicin-GP9.8-DDI-Standard-KS-MBB-SA-RC-2020-12-22.mdb							
Record:	Rifamp 600mg PO DDI PO 3mg MDZ Kharasch							
[NewTable]	Dynamic Simulation Results							
Compound	Fa [%]	FDp [%]	F [%]	Cmax [ug/mL]	Tmax [h]	AUC(0-t) [ng-h/mL]	AUC(0-inf) [ng-h/mL]	
Midaz PO 3.0mg vs RIF 600mg 5d Kharasch-baseline	99.99	27.94	15.15	0.00688	132.7	18.26	20.13	
Rifamp 600mg PO DDI PO 3mg MDZ Kharasch-baseline	99.95	97.86	90.54	12.76	121.6	473000	474000	
RIF-Gluc Metabolite-baseline	0	0	0	1.907	99.64	99900	100000	
Midaz PO 3.0mg vs RIF 600mg 5d Kharasch-DDI	99.99	5.487	0.756	0.00034	132.4	0.524	0.54	
Rifamp 600mg PO DDI PO 3mg MDZ Kharasch-DDI	99.97	86.52	75.92	12.18	1.5	251000	251000	
RIF-Gluc Metabolite-DDI	0	0	0	2.419	3.76	92500	92600	
Midaz PO 3.0mg vs RIF 600mg 5d Kharasch-ratio	1	0.196	0.05	0.05	0.998	0.029	0.027	
Rifamp 600mg PO DDI PO 3mg MDZ Kharasch-ratio	1	0.884	0.839	0.955	0.012	0.531	0.53	
RIF-Gluc Metabolite-ratio	0	0	0	1.268	0.038	0.926	0.926	

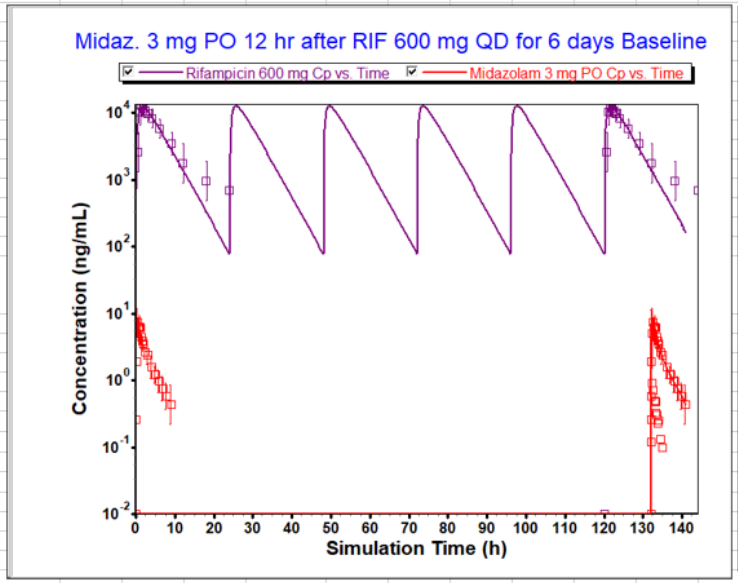

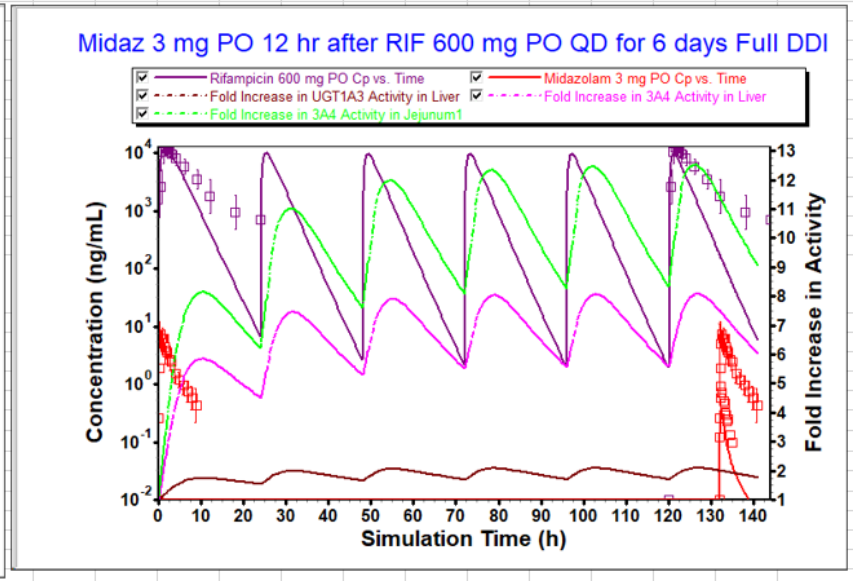

Peloquin 600mg PO Results | Acocella 600mg 900mg PO QD | Acocella 600mg 900mg Results | Kharasch 2011 600mg DDI Alf IV | Khar. 2004 600mg vs Midaz IV | **Khar. 2004 600mg vs Midaz PO**

SimulationsPlus
SCIENCE + SOFTWARE = SUCCESS

Inclusion of a spreadsheet for fast editing of Perpetrator Table with new "Validated" Field

H58 | Ogilvie-Parkinson-DrugMetabDispos-34-1-191-2006-Reversible Inhibition (IC50,t,HLM) of paclitaxel metabolism by gemfibrozil glucuronide in HLM.

	A	B	C	D	E	F	G	H	I	J	K	L	M
1		**Perpetrators Table**											
2	OrigOr	Generic	Enzyme	InhibitionConstant	InhibitionConstantUnits	InhibitionConstantType	Substrate	Reference	InVitroFu	InVitroFuType	InVitroProtConc	Kinact	Validate
84	82	Gem Gluc Tornio EC Kps	2C8	20	uM	IC50-irr-in vitro, T	Paclitaxel	Ogilvie-Parkinson-DrugMetabDispos-34	0.992	Calc(Hallifax)-HLM	0.1	0.21	TRUE
85	83	Gem Gluc Tornio EC Kps	2C8	24	uM	IC50-rev-in vitro, T	Paclitaxel	Ogilvie-Parkinson-DrugMetabDispos-34	0.826	Calc(Hallifax)-HLM	0.5	0	FALSE
86	84	Gem Gluc Tornio EC Kps	OAT3	9.9	uM	Ki-rev-in vitro, U	14C-Pravastatin	Nakagomi-Hagihara-Xenobiotica-37-4-4	-1	Unknown	0.5	0	TRUE
87	85	Gem Gluc Tornio EC Kps	OAT3	13	uM	IC50-rev-in vitro, U	Unknown	Yoshida-ClinPharmTherap-91-6-1053-20	-1	Unknown	0.5	0	FALSE
88	86	Gem Gluc Tornio EC Kps	OATP1B1	22.6	uM	Ki-rev-in vitro, U	3H-Pitavastatin	Hirano-Sugiyama-DrugMetabDispositio	-1	Unknown	0.5	0	FALSE
89	87	Gem Gluc Tornio EC Kps	OATP1B1	15.7	uM	Ki-rev-in vitro, T	14C-Pravastatin	Nakagomi-hagihara-Xenobiotica-37-5-4	0.987	Calc(Austin)-Hep	0.5	0	FALSE
90	88	Gem Gluc Tornio EC Kps	OATP1B1	7.6	uM	Ki-rev-in vitro, U	14C-Pravastatin	Nakagomi-hagihara-Xenobiotica-37-5-4	-1	Unknown	0.5	0	TRUE
91	89	Gem Gluc Tornio EC Kps	OATP1B1	14	uM	IC50-rev-in vitro, U	Unknown	Yoshida-ClinPharmTherap-91-6-1053-20	-1	Unknown	0.5	0	FALSE
92	90	Gem Gluc Tornio EC Kps	OATP1B3	74	uM	IC50-rev-in vitro, U	Unknown	Yoshida-ClinPharmTherap-91-6-1053-20	-1	Unknown	0.5	0	FALSE
93	91	GEM PO 600 mg DDI Repag Tornio	2C8	30.4	uM	Ki-rev-in vitro, T	Paclitaxel	Kajosaari-Backmann-BasicClinPharmcol	0.826	Calc(Hallifax)-HLM	0.5	0	TRUE
94	92	GEM PO 600 mg DDI Repag Tornio	2C8	120	uM	IC50-rev-in vitro, T	Paclitaxel	Ogilvie-Parkinson-DrugMetabDispos-34	0.826	Calc(Hallifax)-HLM	0.5	0	FALSE
95	93	GEM PO 600 mg DDI Repag Tornio	2C9	30	uM	IC50-rev-in vitro, T	Diclofenac	Ogilvie-Parkinson-DrugMetabDispos-34	0.826	Calc(Hallifax)-HLM	0.5	0	FALSE
96	94	GEM PO 600 mg DDI Repag Tornio	2C9	4	uM	Ki-rev-in vitro, U	Tolbutamide	Wang-JPET-302-1-43-2002-Unbound inhi	-1	Unknown	0.5	0	FALSE
97	95	GEM PO 600 mg DDI Repag Tornio	2C9	5.8	uM	Ki-rev-in vitro, T	Tolbutamide	Wen-Neuvoven-DrugMetabDisposition-	0.826	Calc(Hallifax)-HLM	0.5	0	TRUE
98	96	GEM PO 600 mg DDI Repag Tornio	NTCP	23	uM	IC50-rev-in vitro, U	Rosuvastatin	Ho et al-Gastroenterology. 2006-130(6)1	-1	Unknown	0.5	0	FALSE
99	97	GEM PO 600 mg DDI Repag Tornio	OAT3	3.4	uM	Ki-rev-in vitro, U	14C-Pravastatin	Nakagomi-Hagihara-Xenobiotica-37-4-4	-1	Unknown	0.5	0	FALSE
100	98	GEM PO 600 mg DDI Repag Tornio	OAT3	3.2	uM	IC50-rev-in vitro, U	Unknown	Yoshida-ClinPharmTherap-91-6-1053-20	-1	Unknown	0.5	0	FALSE
101	99	GEM PO 600 mg DDI Repag Tornio	OATP1B1	25.2	uM	Ki-rev-in vitro, U	3H-Pitavastatin	Hirano-Sugiyama-DrugMetabDispositio	-1	Unknown	0.5	0	FALSE
102	100	GEM PO 600 mg DDI Repag Tornio	OATP1B1	31.7	uM	Ki-rev-in vitro, T	14C-Pravastatin	Nakagomi-hagihara-Xenobiotica-37-5-4	0.645	Calc(Austin)-Hep	0.5	0	FALSE
103	101	GEM PO 600 mg DDI Repag Tornio	OATP1B1	15.1	uM	Ki-rev-in vitro, U	14C-Pravastatin	Nakagomi-hagihara-Xenobiotica-37-5-4	-1	Unknown	0.5	0	FALSE
104	102	GEM PO 600 mg DDI Repag Tornio	OATP1B1	4	uM	IC50-rev-in vitro, U	3H-Rosuvastatin	Schneck-ClinPharmacolTher-75-5-455-2	-1	Unknown	0.5	0	FALSE
105	103	GEM PO 600 mg DDI Repag Tornio	OATP1B1	12.5	uM	Ki-rev-in vitro, U	3H-E217BETAG	Yamazaki-Lin-Xenobiotica-35-7-737-200	-1	Unknown	0.5	0	TRUE
106	104	GEM PO 600 mg DDI Repag Tornio	OATP1B1	20	uM	IC50-rev-in vitro, U	Unknown	Yoshida-ClinPharmTherap-91-6-1053-20	-1	Unknown	0.5	0	FALSE

For example: the rifampicin perpetrator table has > 400 rows

Documentation directly in comment field of database

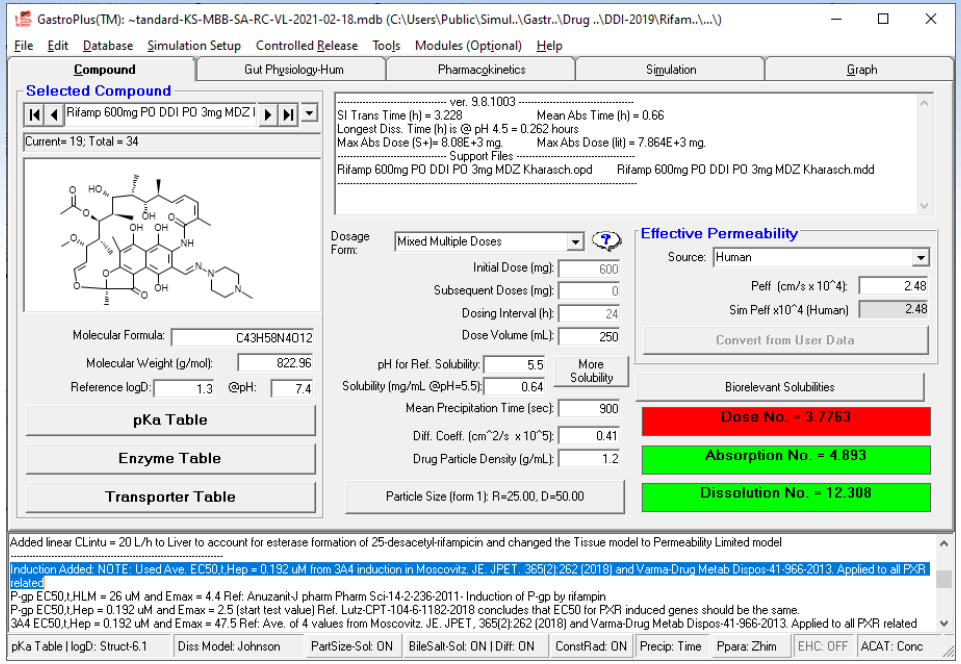

All properties are predictions from ADMET Predictor v9.5.0.0
Tendency Supersaturate=SupSat; Likelihood of BBB Penetration=Low (92%); Pgp-Inhibitor=Yes (97%); Pgp-Substrate=Yes (94%); OATP1B1-Inhibitor=Yes (91%); OCT2-Inhibitor=No (95%); BSEP-Inhibitor=Yes (83%); BCRP-Substrate=Yes (54%);
ECCS Classification=Class_4; High_MWt; S+ Mechanistic Clearance Classification=HepUptake;
Human Rbp prediction saved in database. Predicted Rat Rbp = 1.25
Human Fup prediction saved in database. Predicted Rat Fup = 11.27%

MBB, 4/5/2020, Updated 12/27/2020
Clinical data from
Changed log P to log D(7.4) = 1.3 Ref. Measured in Roche discovery assays: Baneyx-EurJPharmSci-56-1-2014-PBPK modeling of CYP3A4 induction by rifampicin
Used log P = 1.5 to calculate Kps and chnaged back log p= 1.3
Changed Solubility to 0.64 at pH 5.5 Ref. Becker-J Pharm Sci-98-7-2252-2009-Rifampicin Biowaiver monograph- pH Vs Solubility profile
Roche PAMPA based conversion to Peff = 0.4E-4 cm/s (a value determined from PAMPA. Ref. Measured in Roche discovery assays: Baneyx-EurJPharmSci-56-1-2014) was increased by 6.2-Fold to 2.48E-4 cm/s per Baneyx for all records.
Changed fup% = 7% Ref. Yoshikado-ClinPharmTherap-100-5-513-2016-Supplement
Changed Rbp = 0.8 to calculate Kps that match the Noncompartmental Vdss for healthy subjects.
etc.

Induction Added: NOTE: EC50.u = 64 nM Unbound 3A4 induction from Asaumi R, CPT Pharmacometrics Syst. Pharmacol. 7: 186 (2018). Applied to all PXR related genes.
P-gp EC50,t,HLM = 26 uM and Emax = 4.4 Ref: Anuzanit-J pharm Pharm Sci-14-2-236-2011- Induction of P-gp by rifampin
P-gp EC50,t,Hep = 0.064 uM and Emax = 2.2 Ref. Lutz-CPT-104-6-1182-2018 concludes that EC50 for PXR induced genes should be the same.
etc.
UGT1A1 EC50,t,Hep = 0.0.64 uM and Emax = 4.4 Emax is the average of 3 values from Moscovitz (Note: Same Emax as UGT2B7 which are in both Gut and Liver Ref. Moscovitz, 2018
etc.

Inhibition Added:
P-gp inhibition Ki,t,HLM = 13.7 uM Substrate E17G and NMQ Ref. for HEK293 iinverted memb. vessicles Ave. Pedersen-EurJPharmSci-103-70-2017
OATP1B1 inhibition Ki = 0.62 uM Substrate = 3H-TIC Ref. Takashima T. J. Nucl. Med. 53:741 (2012)
3A4 inhibition Ki,u = 18.5 uM Ref. Kajosaari-BasicClinicalPharmacolToxicol-97-249-2005
etc.

Biotransformation Pathway of Gemfibrozil

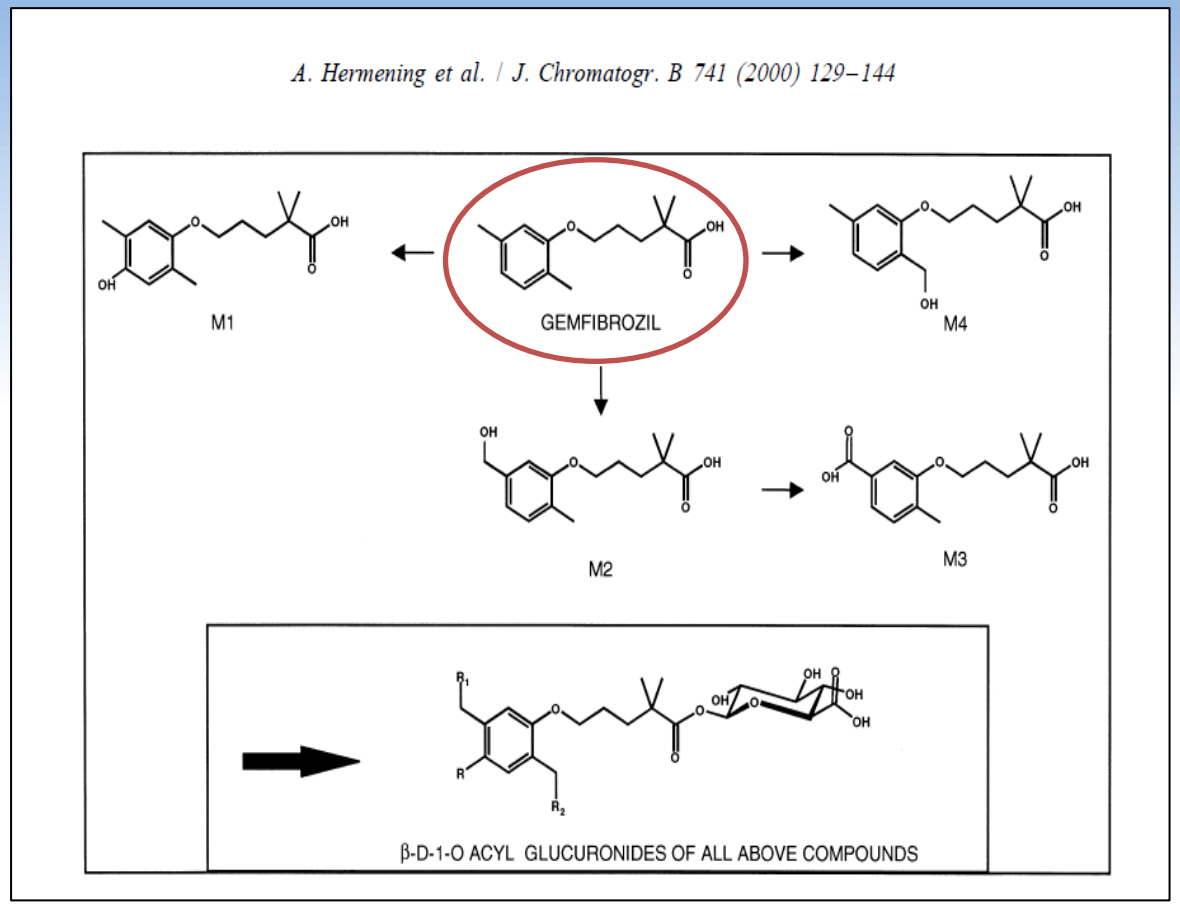

Excretion balances (% of dose) of gemfibrozil and its phase-I and phase-II metabolites in young hyperlipidaemic patients after oral administration of a single gemfibrozil dose (900 mg)[a]

	Urinary recovery (% of dose)	
	Aglycones	Acyl glucuronides
Gemfibrozil	0.04±0.01	34.1±8.9
Metabolite 1	0.02±0.01	5.0±1.7
Metabolite 2	–	1.1±0.2
Metabolite 3	9.6±2.4	15.1±2.9
Metabolite 4	–	0.6±0.1
Total	9.6±2.4	55.9±11.5

[a] Amounts excreted into urine extrapolated to infinity were calculated as $Ae_{0\to\infty} = Ae_{0\to t_{last}}/(1 - e^{-\lambda z \cdot t_{last}})$. (All values are expressed as mean±SD; $n = 3$.)

Hermening et al., J. Chromatogr. B. BiomedSci.741(2) :129 (2000)

Elimination of Gemfibrozil-^{3}H in Human

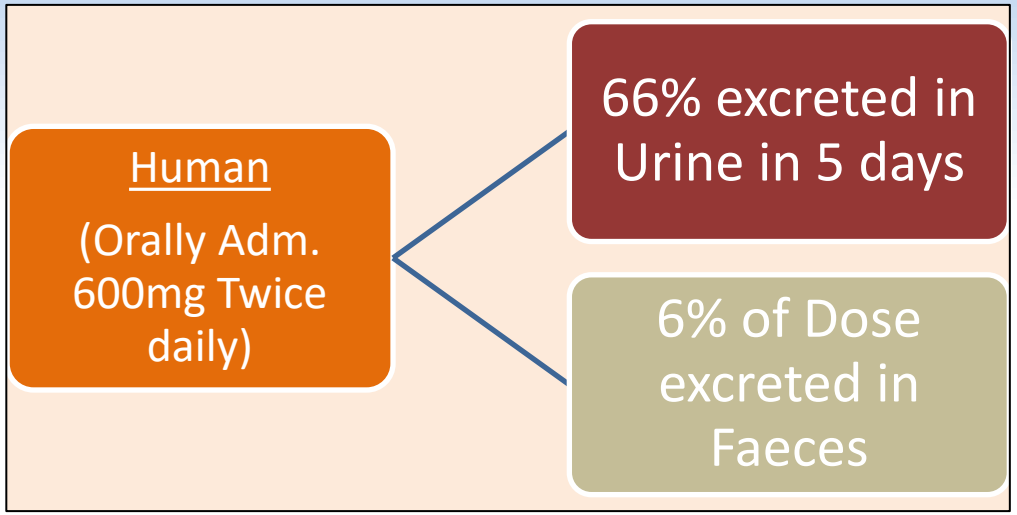

Table I

Fractionation of 0–48 h urinary tritium obtained from 6 human subjects maintained on a 600 mg twice daily dose schedule

	Percentage of dose		
Metabolite	*Unconjugated*	*Conjugated*	*Total*
Gemfibrozil	0.26	30.36	30.62
Metabolite I	0.07	1.40	1.47
Metabolite II	0.00	1.65	1.65
Metabolite III	6.95	5.02	11.97
Metabolite IV	0.00	6.78	6.78
Total	7.28	45.21	52.49 ●

● Total non-volatile tritium recovery in the 0–48 h urine collections = 63.6%

Okerholm et al. Proc. Roy. Soc. Med. 29 (2):11 (1976)

Mechanism of CYP2C8 inhibition by Gemfibrozil

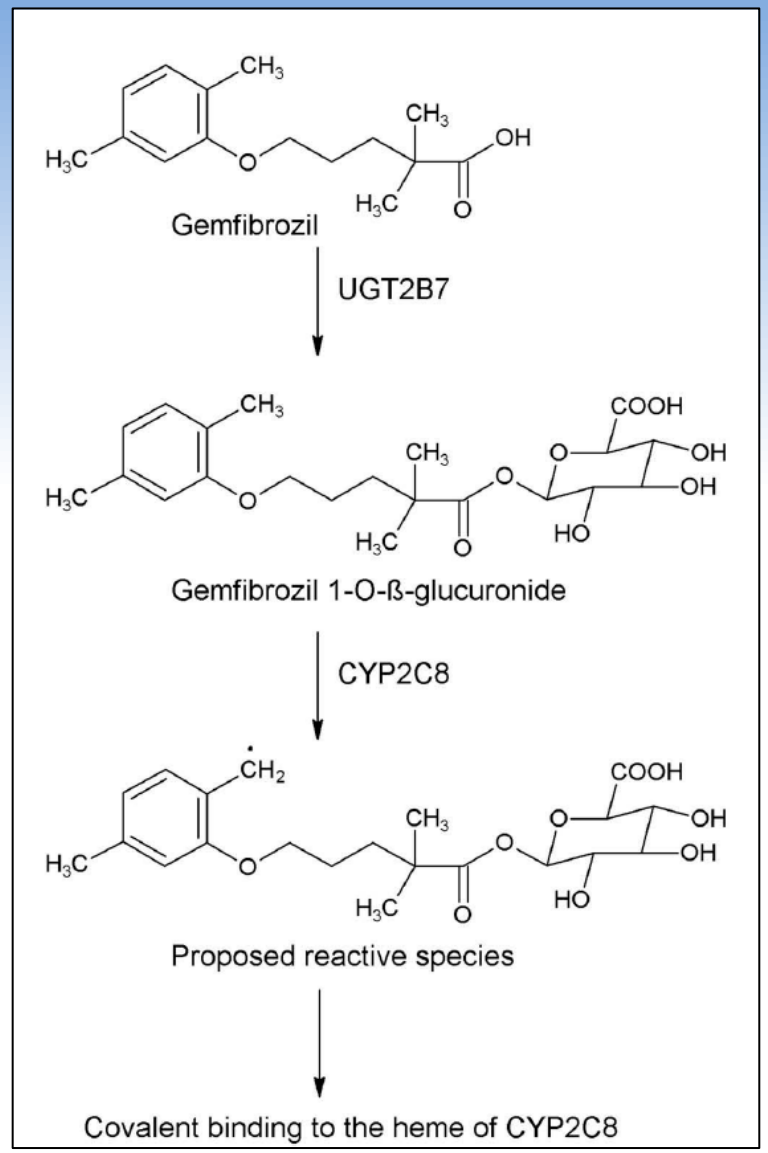

Glucuronidation converts Gemfibrozil to a mechanism-based inhibitor of CYP2C8 resulting in an irreversible inhibition.

Tornio-Backman-Exp.Opin. Drug Metab. Toxicol. 13(1):83 (2017)

Ogilvie et al. Drug. Metab. Dispos. 34(1):191 (2006)

Overview of Gemfibrozil ADME in Humans

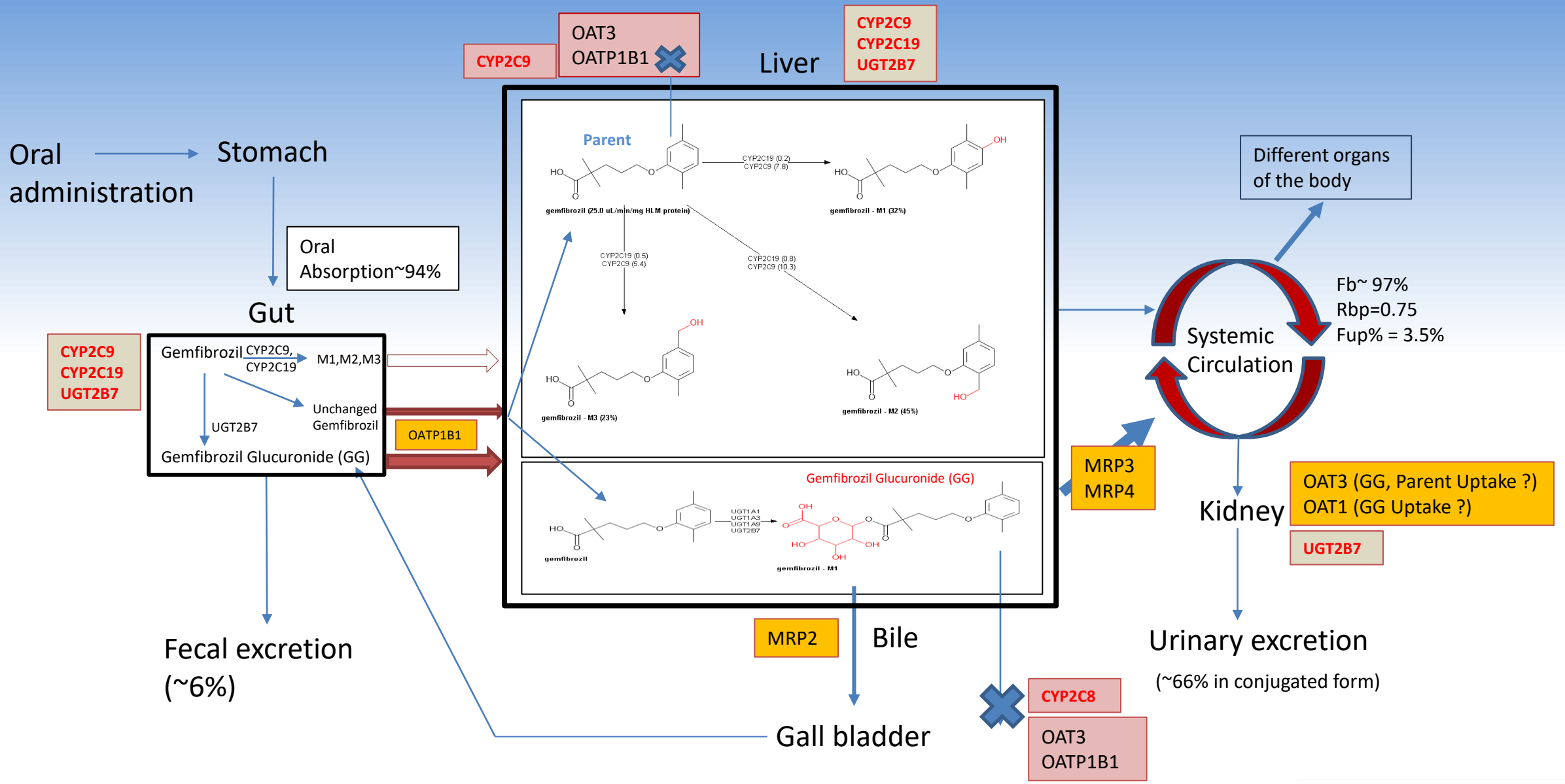

Figure by Saima Subhani

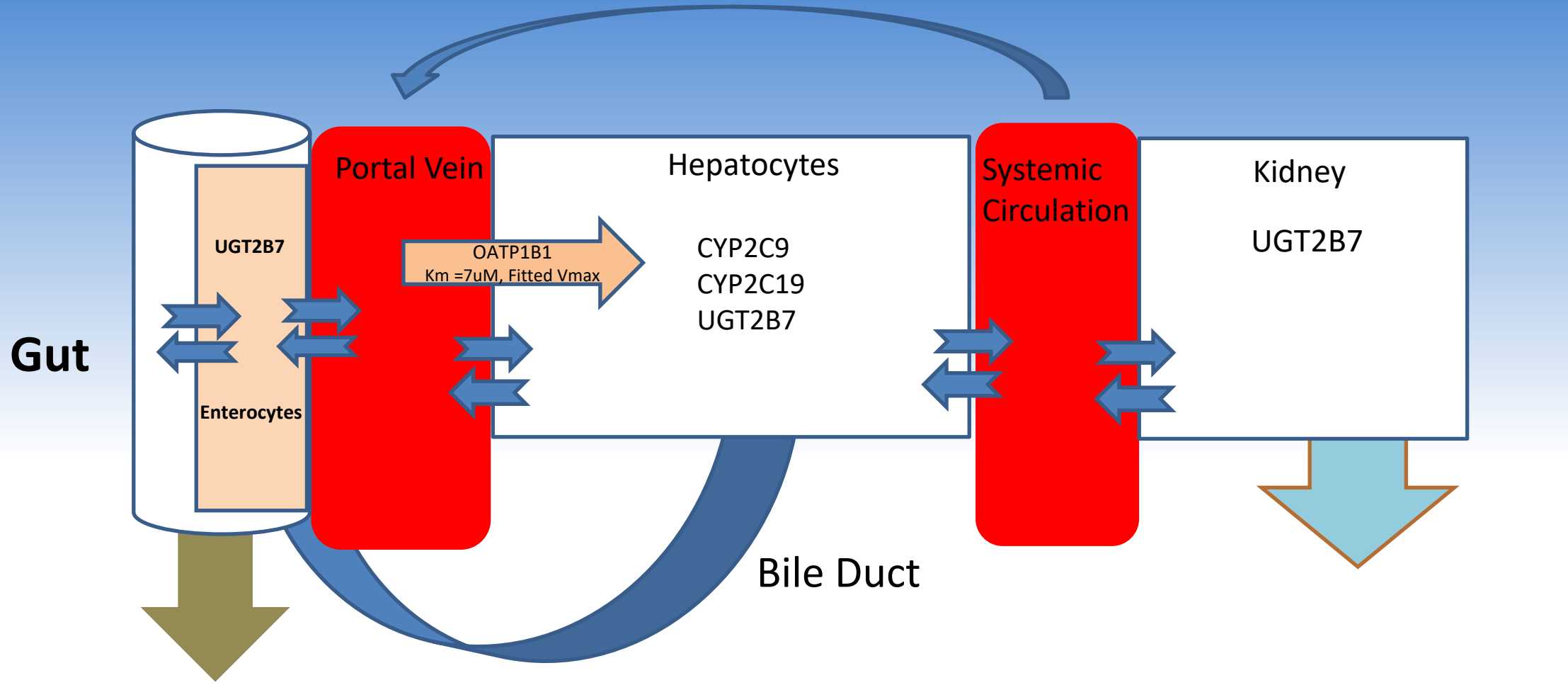

Parent- Gemfibrozil

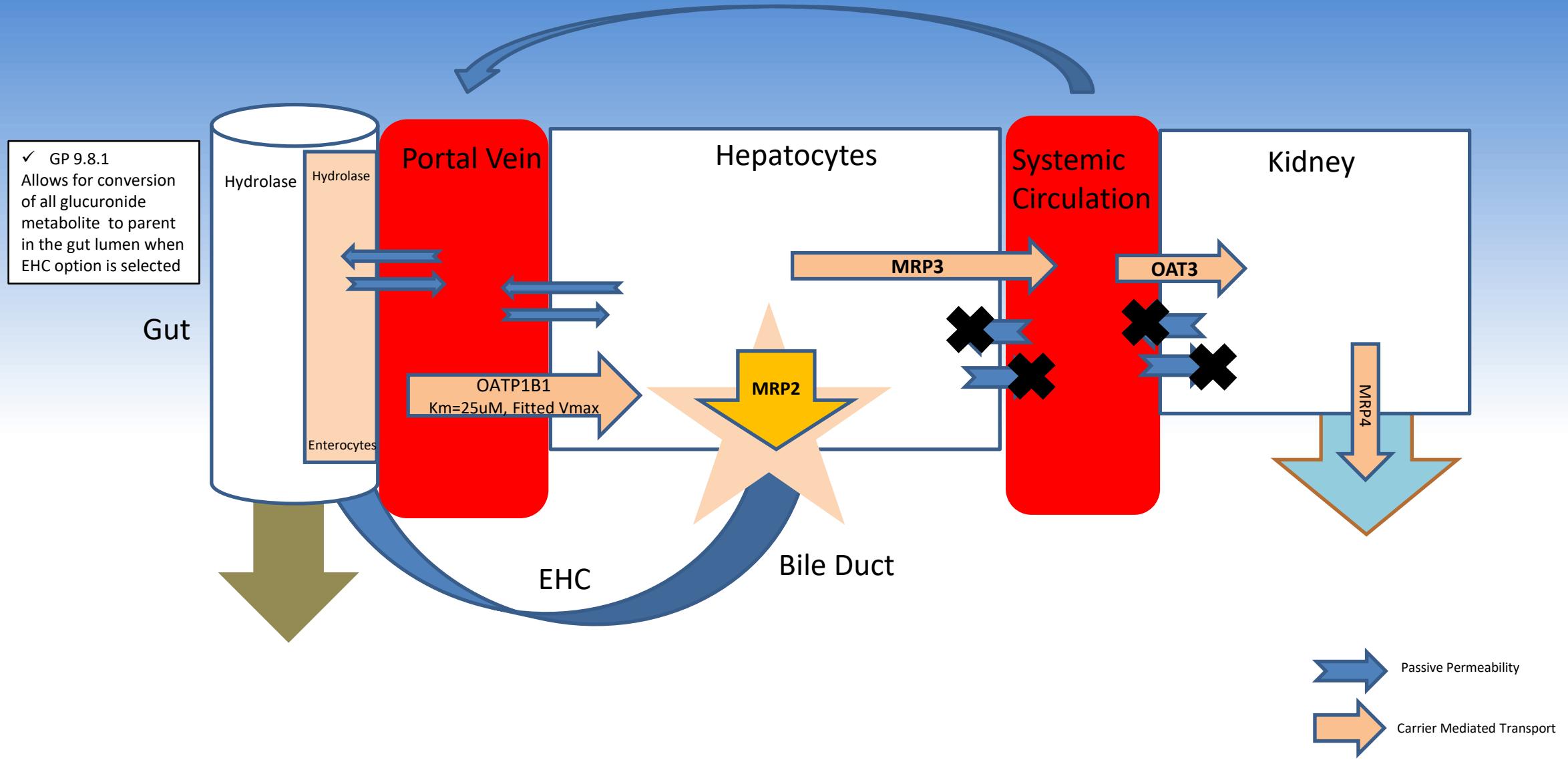

Metabolite- Gemfibrozil Glucuronide

Acyl-glucuronide Conversion to Parent in Gut Lumen

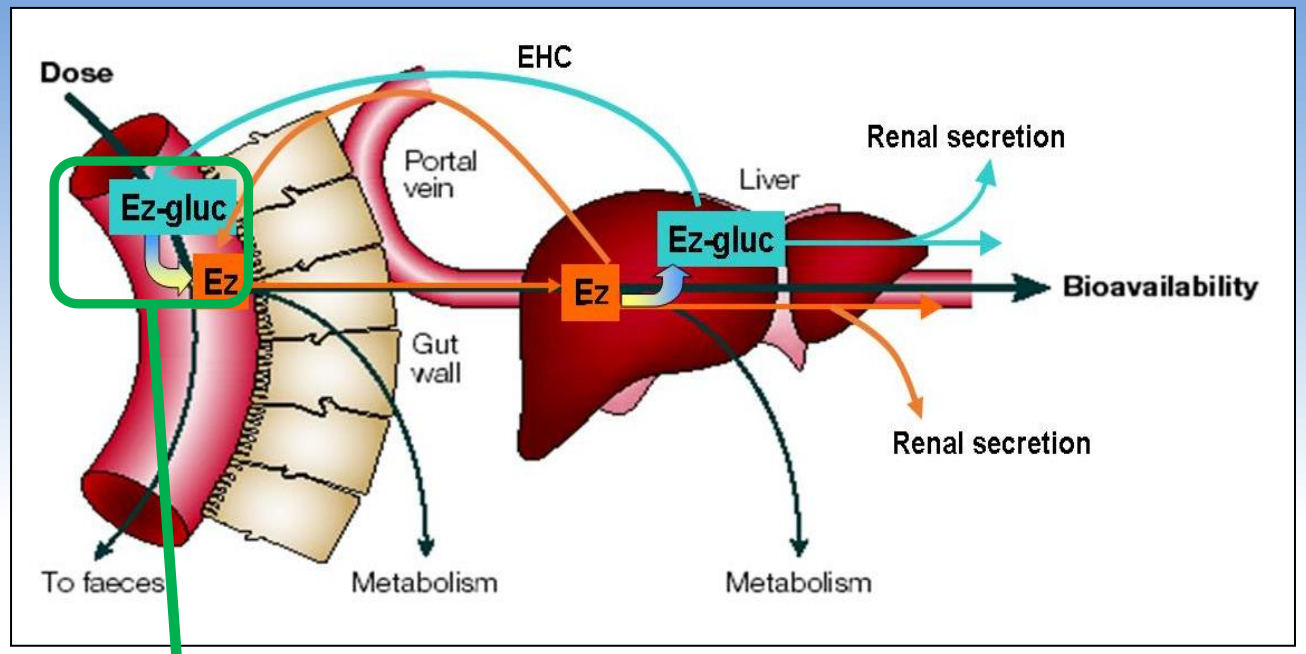

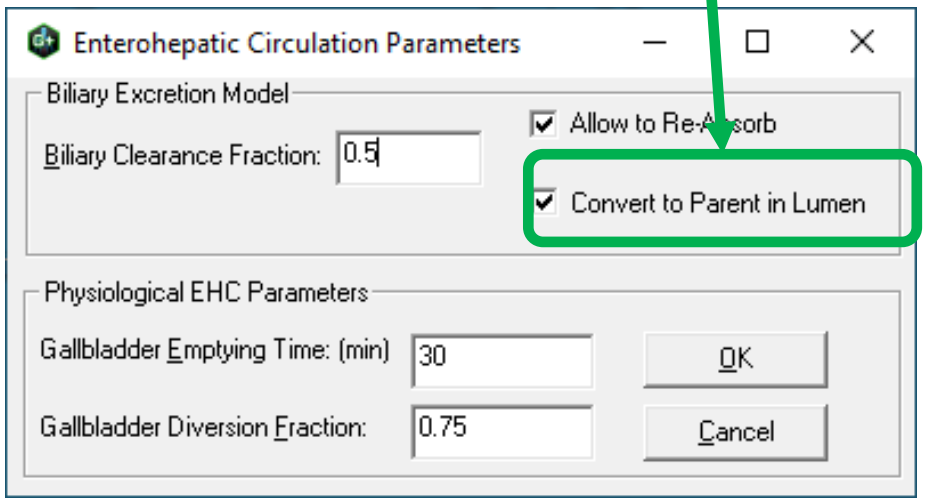

- This is not a general solution for compound metabolism in gut lumen (that is coming in GPX)
- It is applicable primarily for acyl-glucuronide metabolites
- It produces parent compound in the lumen for re-absorbtion
- Assumes breakdown of glucuronides so molecular ratio = 1

Outline of Process for Model Development and Documentation

- Creation of GP a project starts with structure import using ADMET Predictor Module for both substrates and perpetrators.
  - Physicochemical, biopharmaceutical, and biochemical properties
  - Initial evaluation via “Chemistry Classification” with all aspects of ADMET
    - Solubility vs. pH, dissolution, absorption (w/ influx and efflux transporters), clearance (metabolic, biliary, and renal), distribution, excretion, and toxicity.
  - Extensive literature collection and spreadsheet documentation.
    - Workbook with multiple sheets for Physicochemical, Metabolic, Transporter, Preclinical, and Clinical single compound and DDI study data for multiple perpetration mechanisms.
  - First simulations for “Measured Properties” with parameter sensitivity analysis.
  - Model building for individual substrate and/or perpetrator simulations compared to observed data for single escalating doses (for nonlinear dose dependence), multiple dosing (for autoinhibition / autoinduction).
  - DDI simulations for all appropriate mechanisms on both substrate and perpetrator.
  - Analysis of results using the “Guest”* criterion for different levels of accuracy cutoff for increasing AUC (inhibition) and decreasing AUC (induction).
  - Preparation of slides and written reports suitable for regulatory submission.

Midazolam BCS/BDDCS II Physicochemical Properties

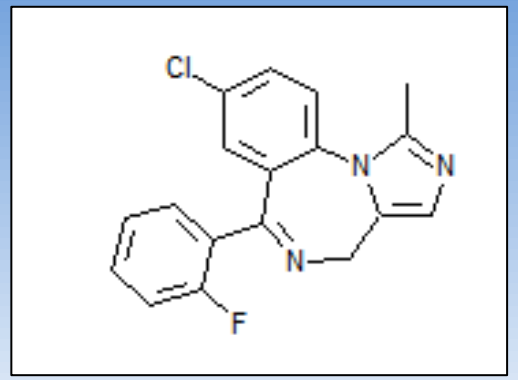

MW = 325.77

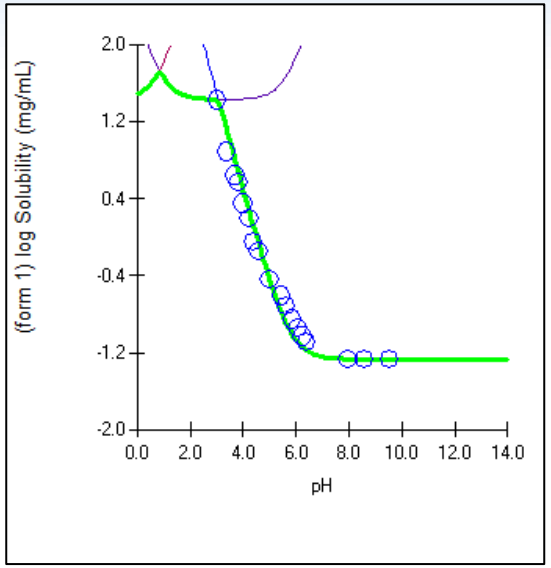

AP 9.5 = ADMET Predictor v. 9.5
S+ = properties predicted with Simulations Plus models
S+Sw = native solubility in pure water
S+Peff = human jejunal permeability estimate

S+LogP = 3.56 (AP 9.5)
Exp LogP = 2.7 (Hoffmann-La Roche)

S+pKa = 4.57 (Base) and 0.84 (Base
Exp pKa = 6.04 (Andersin-JPharmaceutBioMedAnal-9-6-451-1991)

S+Sw = 2.1 μg/mL @ pH = 7.05 (AP 9.5)
Exp Sw = 54 μg/mL @ pH 9.5 Andersin, 1991) LOW

S+FaSSIF = 33 μg/mL, S+ FeSSIF = 210 μg/mL
Exp FaSSIF = 11 μg/mL, (personal communication ??)

S+Peff = 7.55 x 10^{-4} (cm/s) (AP 9.5) HIGH
Exp Ussing Papp = 3.8E-5 cm/s (Sjoberg-Ungel, 2013)
Conversion to Hum. Jej. Peff = 3.82E-4 cm/s

S+HLM-3A4 Km = 21 μM Vmax = 3.5 nmol/min/mg Prot. (AP 9.5)
Exp CYP3A4 Km = 3.7 μM (Paine, 1997)
Exp CYP3A4 Vmax = 0.85 nmol/min/mg Prot.
Exp CYP3A4 Km = 2.27 mM (Walsky, 2004)
Exp CYP3A4 Vmax = 1.22 nmol/min/mg Prot.

S+hum_fup% = 6.61 (AP 9.5)
Exp. Fup = 4.4% Ave. (de Vries, 199) and (Fisher, 1999)

S+RBP = 0.78 (AP 9.5)
Exp Rbp = 0.55 (Gertz, 2011)

Papp to Peff Conversion for Ungel Human Ussing Chamber

Compound	Hum_Peff (cm/s x 10^4	Ussing_Papp (cm/s x 10^5
Antipyrine	5.6	4.97
Atenolol	0.2	0.411
Cimetidine	0.26	0.37

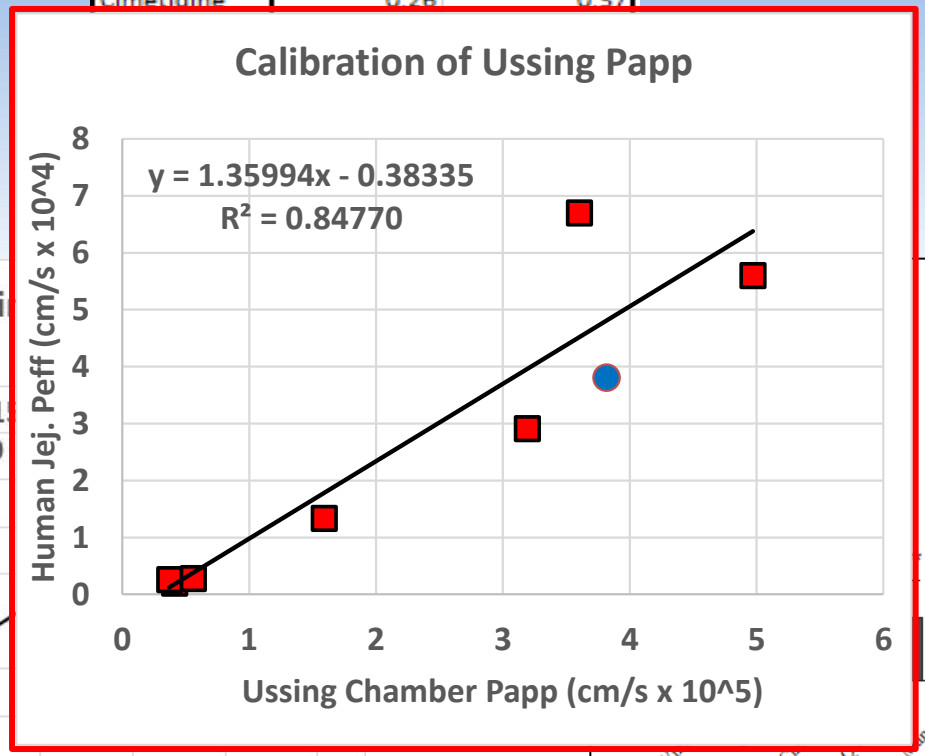

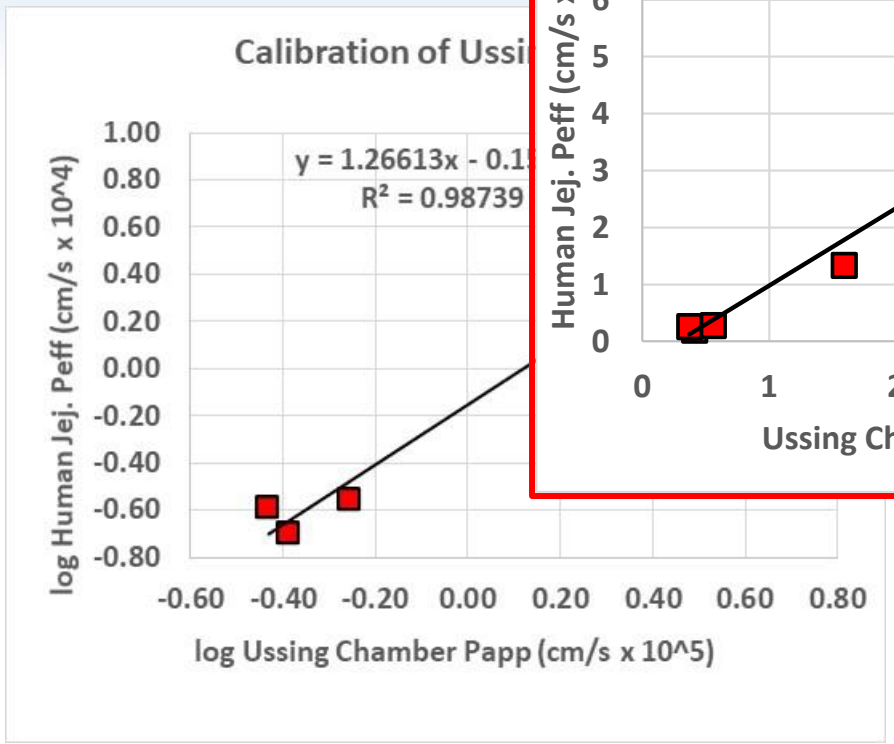

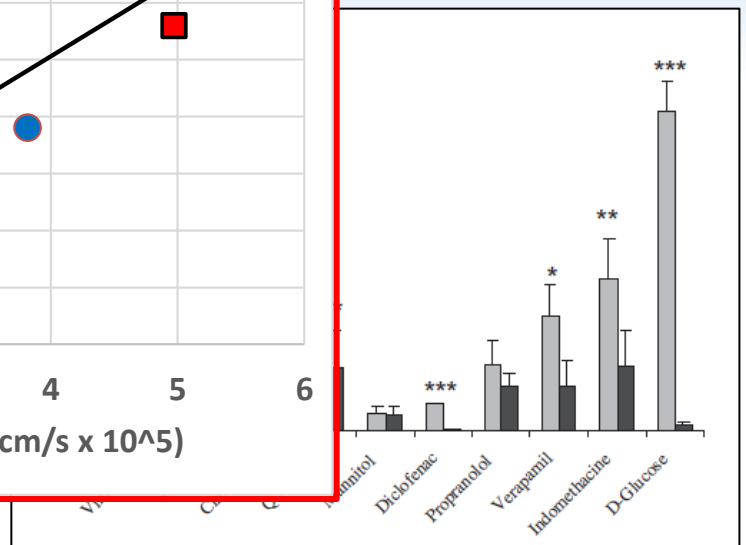

Fig. 5. Bidirectional permeability in human jejunal tissue of transporter dependent compounds (P_{app} *m–s/s–m*) ($\times 10^{-6}$ cm/s) vinblastine (1.31/5.55, $n = 4$), digoxin (1.44/7.79, $n = 7$), cimetidine (3.74/6.68, $n = 5$), quinidine (3.36/19.6, $n = 5$), diclofenac (8.55/0.34, $n = 2$), verapamil (36.0/14.0, $n = 4/3$) and indomethacine (48.2/19.9, $n = 4$). Non transport dependent control compounds mannitol (5.56/4.72, $n = 253/68$), propranolol (20.6/13.7, $n = 2$) and uptake transported D-glucose (101/1.78, $n = 2$). Error bars indicate standard deviation from the mean.

Papp to Peff Conversion for Caco-2 Papp

Compound	Hum_Peff (cm/s x 10^4	Ussing_Papp (cm/s x 10^5	Caco-2 (cm/s x 10^5)	Hum_Peff (cm/s x 10^4
Antipyrine	5.6	4.97	6.34	5.6
Atenolol	0.2	0.411	0.019	0.2
Cimetidine	0.26	0.37	0.027	0.26
Mannitol	0.28	0.556	0.044	0.28
Metoprolol	1.34	1.59	1.17	1.34
Propranolol	2.91	3.19	1.8	2.91
Verapamil	6.7	3.6		6.7
LinMidaz	3.99	3.8	4.74	4.48
Midazolam	3.82	3.8	4.74	4.20

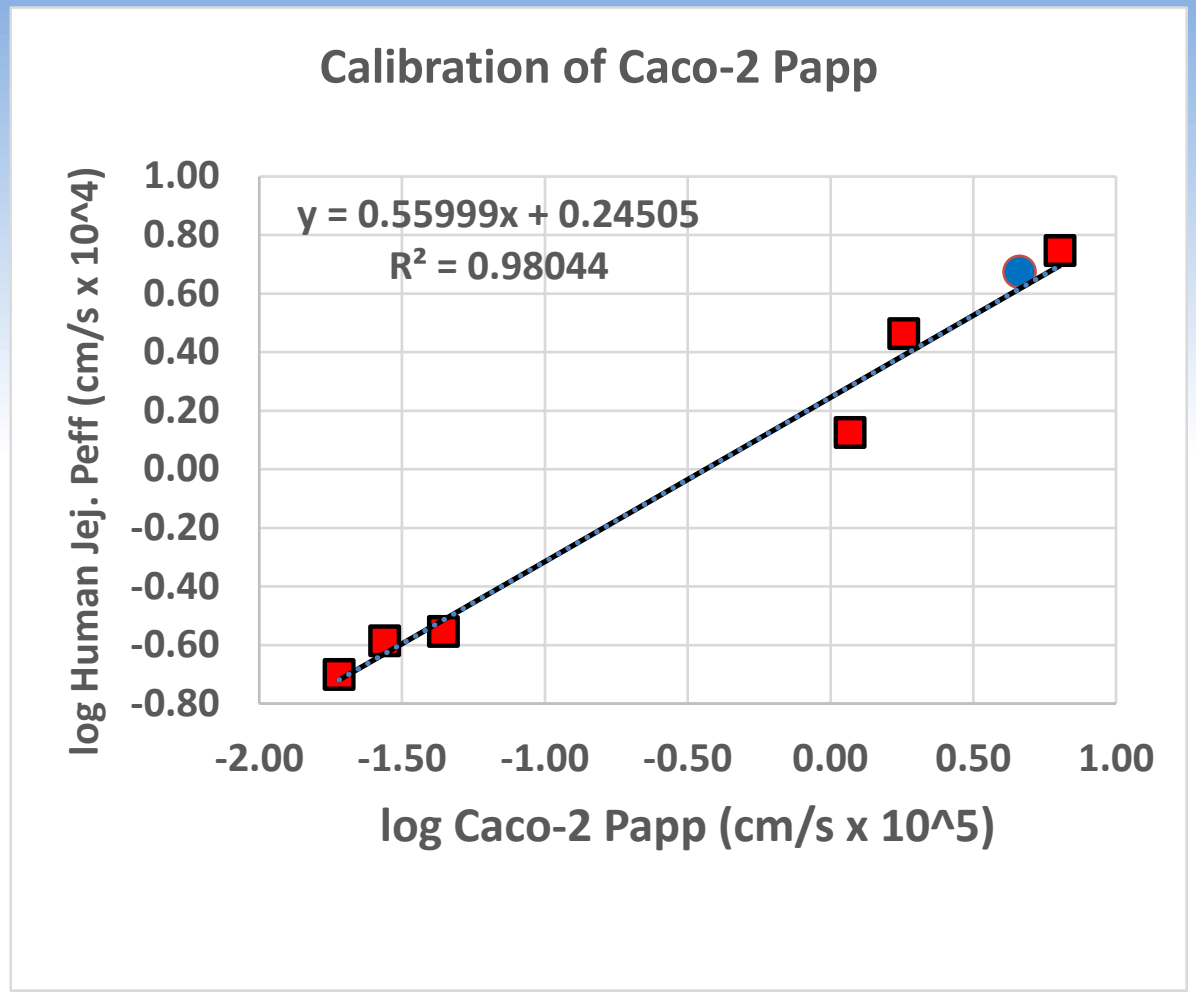

Initial Model for Midazolam 7.5 mg PO Solution Bornemann

- **Assumptions:**
  - Perfusion-limited midazolam
  - Permeability-limited liver and kidney for 1-OH-midazolam
  - Added MRP3 liver basolateral to efflux metabolite to systemic circulation for PO records only.
  - fu_{ent} = 100%
- **Clearance:**
  - Paine-J. Pharmacol. Exp. Ther., 283:1552 (1997) unbound K_m = 3.7 µM and V_{max} = 0.85 nmol/min/mg micro. Prot.
- **Distribution:**
  - Midazolam Lukacova default Kp calculation
  - 1-OH-midazolam reduced log P = 2.2 to calc. Kps and then ran simulation with log P = 2.57

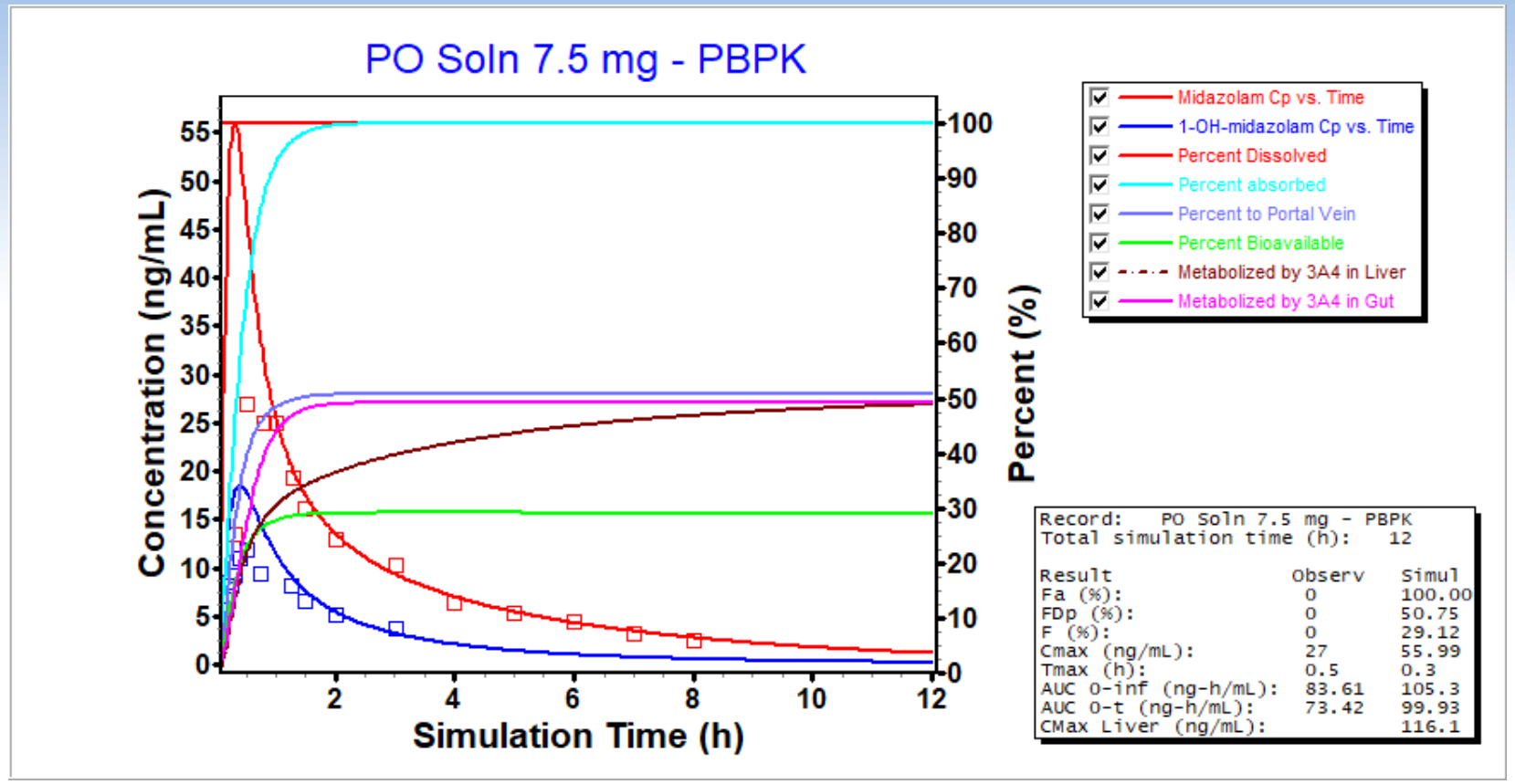

Clinical data from:
Bornemann-EurJClinPharmacol-29-1-91-1985

Midazolam Binds to Fatty Acid Binding Proteins in Gut and Liver

ABSTRACT

Purpose Several poorly water-soluble drugs have previously been shown to bind to intestinal (I-FABP) and liver fatty acid binding protein (L-FABP) *in vitro*. The purpose of this study was to examine the potential role of drug binding to FABPs on intestinal permeability and gut wall metabolism *in vivo*.

Methods The intestinal permeability of ibuprofen, progesterone and midazolam (which bind FABPs) and propranolol (which does not) was examined using an autoperfused recirculating permeability model in control rats and rats where FABP levels were upregulated via pre-feeding a fat-rich diet.

Results The intestinal permeability of drugs which bind FABPs *in vitro* was increased in animals where FABP levels were upregulated by prefeeding a high fat diet. The gut wall metabolism of midazolam was also reduced in animals with elevated FABP levels.

Conclusions Consistent with their role in the cellular transport of endogenous lipophilic substrates, FABPs appear to facilitate the intracellular disposition of drug molecules that bind FABPs *in vitro*. Drug binding to FABPs in the enterocyte may also attenuate gut wall metabolism in a manner analogous to the reduction in hepatic extraction mediated by drug binding to plasma proteins in the systemic circulation.

Pharm Res (2011) 28:2176–2190
DOI 10.1007/s11095-011-0446-1

RESEARCH PAPER

Fatty Acid Binding Proteins: Potential Chaperones of Cytosolic Drug Transport in the Enterocyte?

Natalie L. Trevaskis • Gary Nguyen • Martin J. Scanlon • Christopher J. H. Porter

extraction ratio (Table V). It seems likely, therefore, that midazolam binding to FABP in the enterocyte promoted uptake into the cell but reduced drug access to intracellular metabolic enzymes via a reduction in the intracellular free concentration.

drug molecules that bind FABPs *in vitro*. The extent of gut wall metabolism of midazolam is also reduced in animals with elevated FABP levels, suggesting that drug binding to FABPs in the enterocyte may attenuate gut wall metabolism in a manner analogous to the reduction in hepatic extraction mediated by drug binding to plasma proteins in the systemic circulation. Finally, it should be noted that the

PBPK Model for Midazolam 7.5 mg PO Solution Bornemann

- **Assumptions:**
  - Perfusion-limited midazolam
  - Permeability-limited liver and kidney for 1-OH-midazolam
  - Added MRP3 liver basolateral to efflux metabolite to systemic circulation for PO records only.
  - fu_{ent} = 4.4%
- **Clearance:**
  - Paine-J. Pharmacol. Exp. Ther., 283:1552 (1997) unbound K_m = 3.7 µM and V_{max} = 0.85 nmol/min/mg micro. Prot.
- **Distribution:**
  - Midazolam Lukacova default Kp calculation
  - 1-OH-midazolam reduced log P = 2.2 to calc. Kps and then ran simulation with log P = 2.57

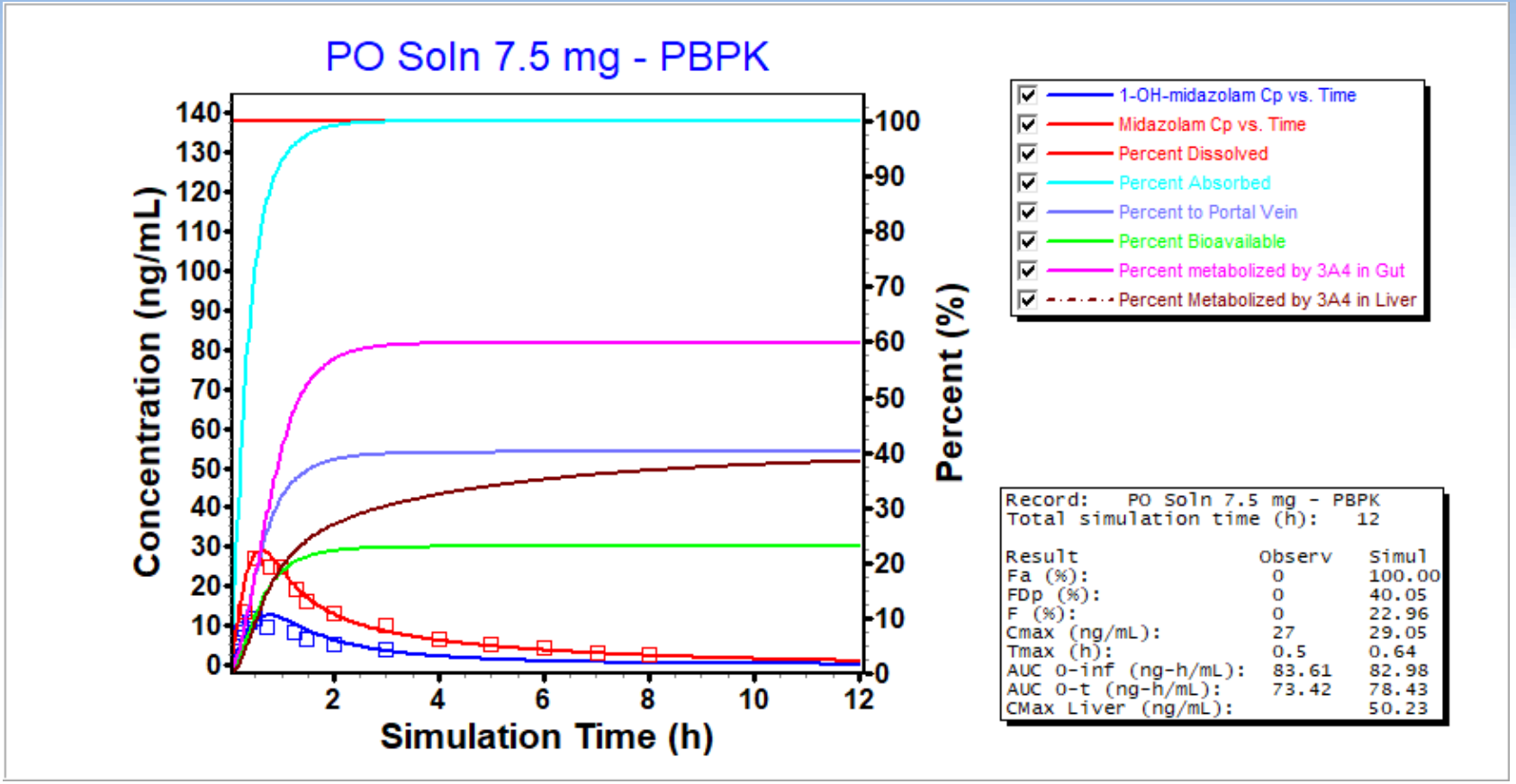

Clinical data from:
Bornemann-EurJClinPharmacol-29-1-91-1985

PBPK Model for Midazolam 15 mg PO Solution Bornemann

- **Assumptions:**
  - Perfusion-limited midazolam
  - Permeability-limited liver and kidney for 1-OH-midazolam
  - Added MRP3 liver basolateral to efflux metabolite to systemic circulation for PO records only.
  - fu_{ent} = 4.4%
- **Clearance:**
  - Paine-J. Pharmacol. Exp. Ther., 283:1552 (1997) unbound K_m = 3.7 µM and V_{max} = 0.85 nmol/min/mg micro. Prot.
- **Distribution:**
  - Midazolam Lukacova default Kp calculation
  - 1-OH-midazolam reduced log P = 2.2 to calc. Kps and then ran simulation with log P = 2.57

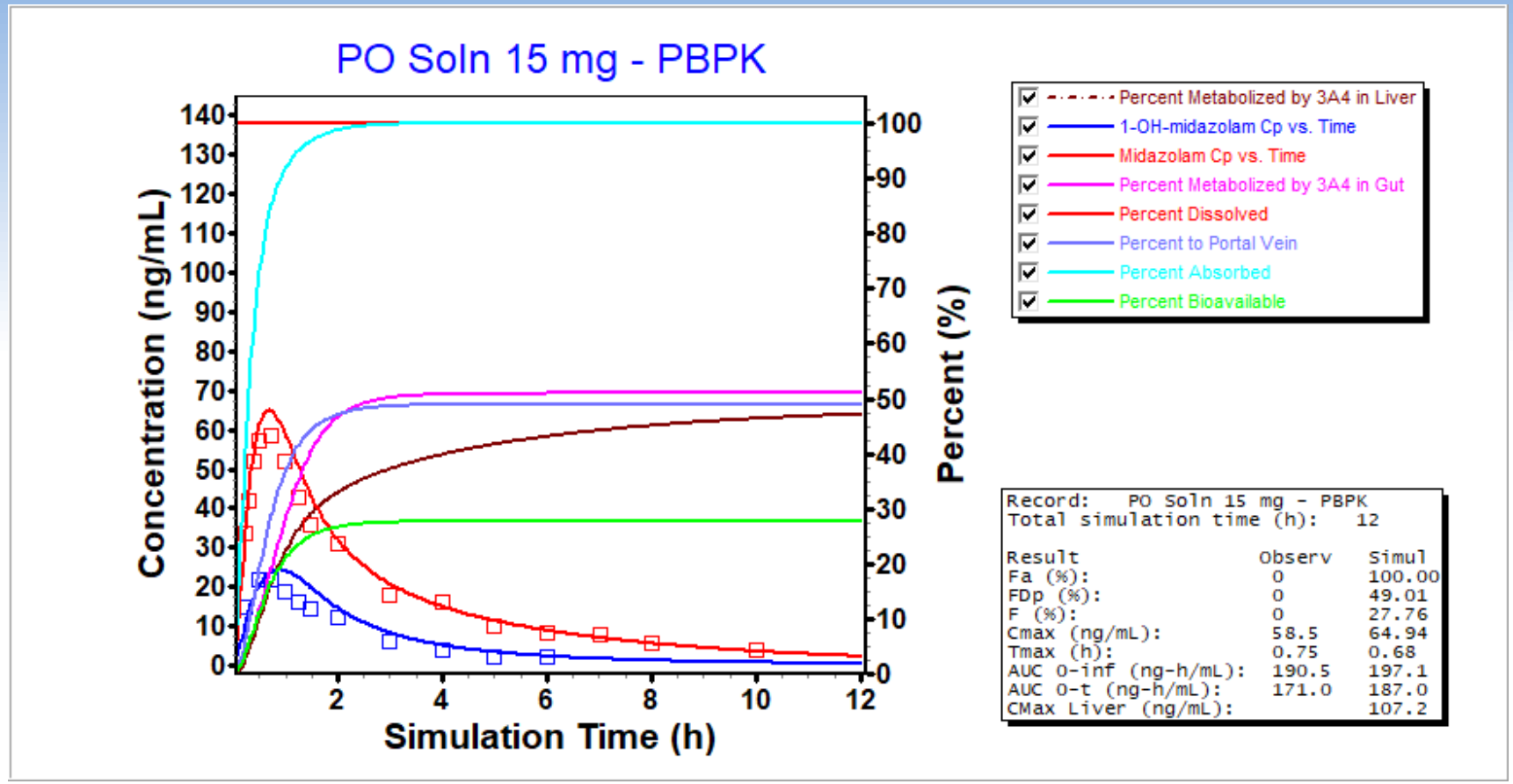

Clinical data from:
Bornemann-EurJClinPharmacol-29-1-91-1985

PBPK Model for Midazolam 30 mg PO Solution Bornemann

- **Assumptions:**
  - Perfusion-limited midazolam
  - Permeability-limited liver and kidney for 1-OH-midazolam
  - Added MRP3 liver basolateral to efflux metabolite to systemic circulation for PO records only.
  - fu_{ent} = 4.4%
- **Clearance:**
  - Paine-J. Pharmacol. Exp. Ther., 283:1552 (1997) unbound K_m = 3.7 µM and V_{max} = 0.85 nmol/min/mg micro. Prot.
- **Distribution:**
  - Midazolam Lukacova default Kp calculation
  - 1-OH-midazolam reduced log P = 2.2 to calc. Kps and then ran simulation with log P = 2.57

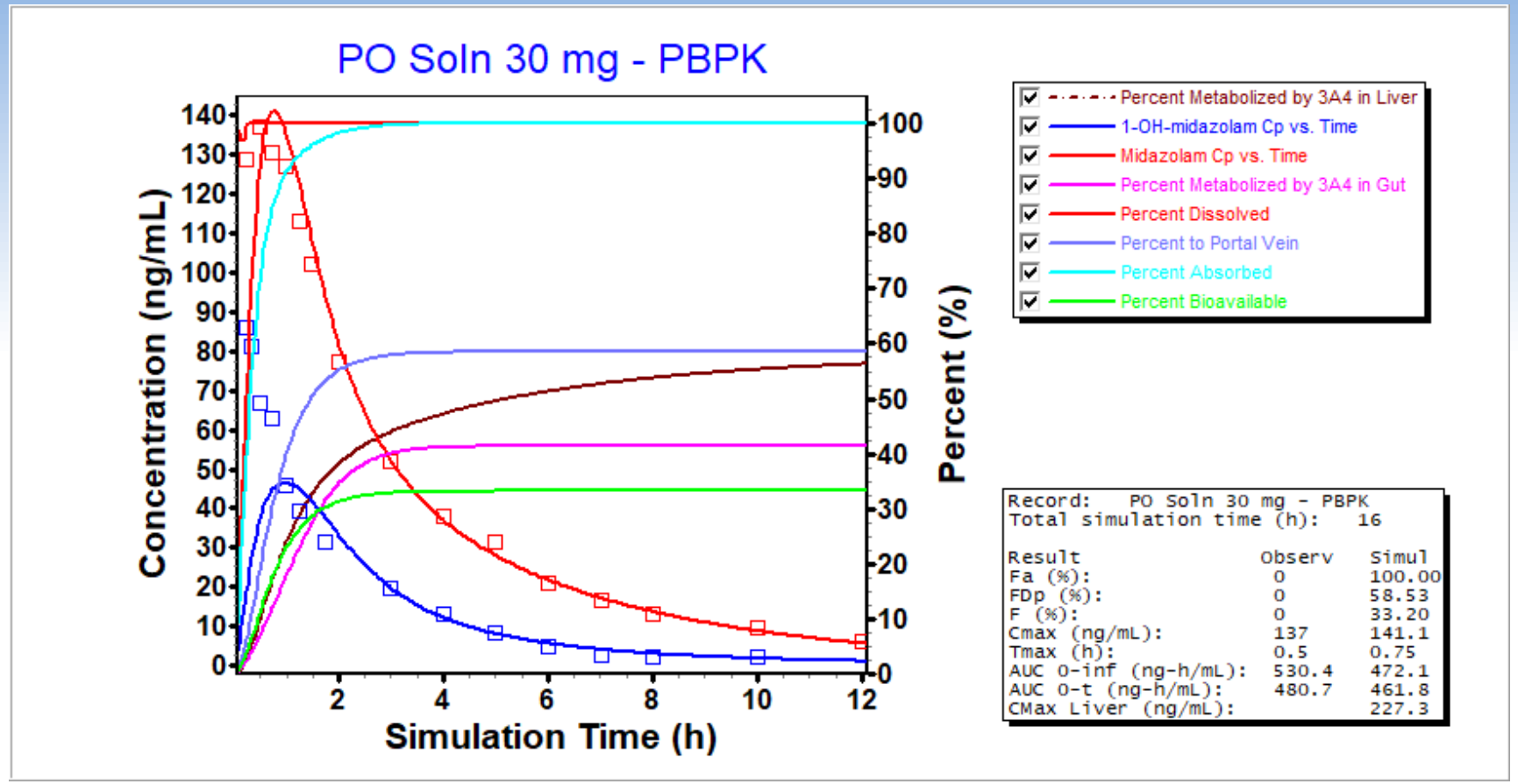

Clinical data from:
Bornemann-EurJClinPharmacol-29-1-91-1985

Midaz. 7.5 mg PO Tab DDI vs. Keto. 400 mg QD for 4 days: Olkkola

Baseline Simulation without DDI interactions

- **Assumptions:**
  - Perfusion-limited midazolam
  - Permeability-limited liver and kidney for 1-OH-midazolam
  - Ketoconazole: 3A4 total Rev. IC_{50} = 26 nM, 3A4 total Irrev. IC_{50} = 15 nM, Kinact = 0.001 min^{-1} and P-gp total IC_{50} = 5.6 μM
  - Reduced fu_{ent} = 4.4% (Ref. Trevaskis-PharmRes-28-9-2176-2011)
- **Clearance:**
  - Paine-J. Pharmacol. Exp. Ther., 283:1552 (1997) unbound $K_{m,u}$ = 3.7 μM and V_{max} = 0.977 nmol/min/mg micro. Prot. The 1.15-fold higher clearance was used due to the Olkkola population of 7 females and 2 male subjects.
- **Distribution:**
  - Midazolam Lukacova default Kp calculation
  - 1-OH-midazolam reduced log P = 2.2 to calc. Kps and then ran simulation with log P = 2.57

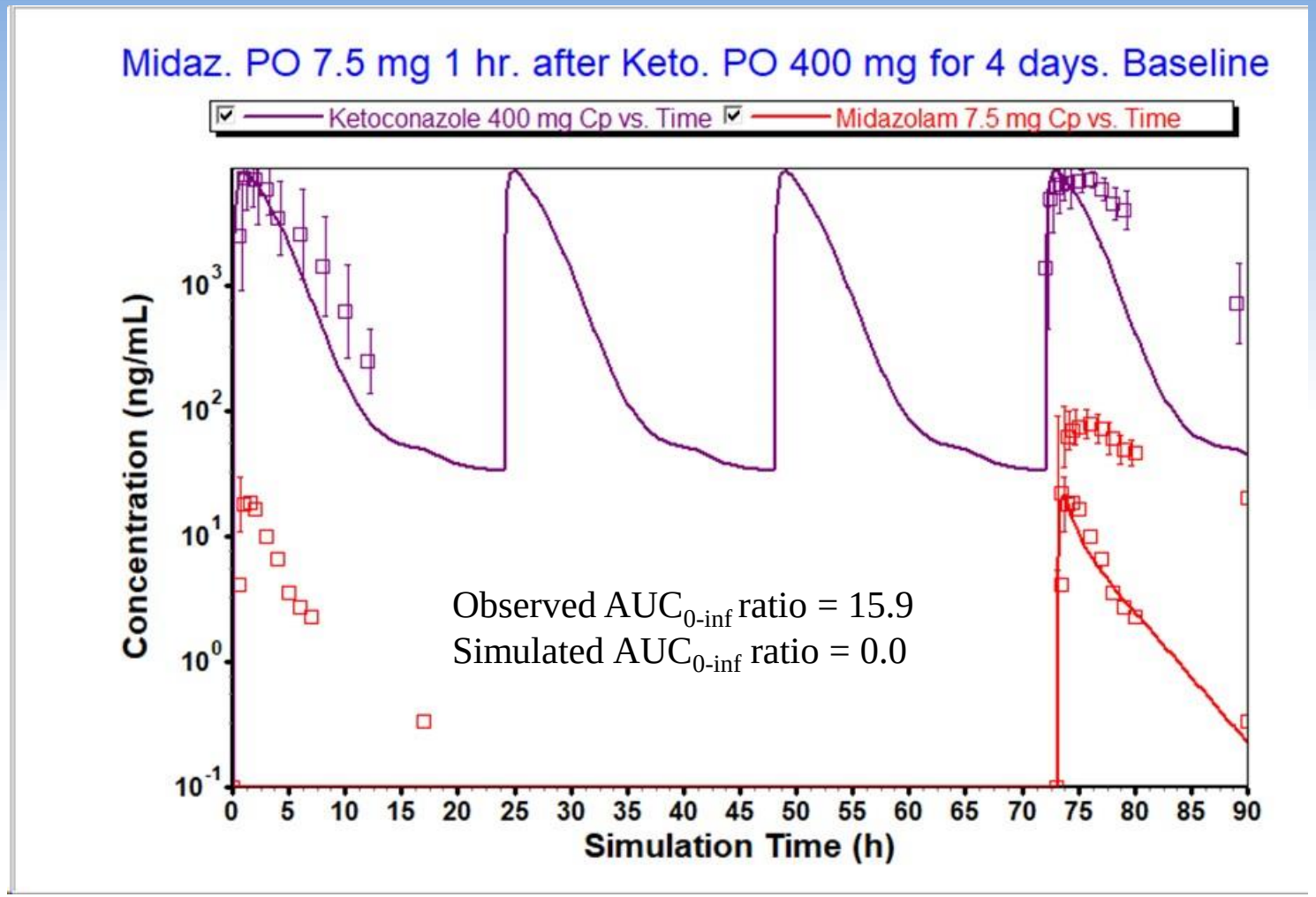

Midazolam clinical data from: Olkkola-ClinPharmacolTherap-55-5-481-1994
Ketoconazole clinical data from: Daneshmend-Antimicrobial agents and Chemotherapy-25-1-1-1984 and Olkkola-ClinPharmacolTherap-55-5-481-1994
Ketoconazole TDI parameters from: Haarhoff-Xenobiotica-47-6-470-2017

Midaz. 7.5 mg PO Tab DDI vs. Keto. 400 mg QD: Olkkola

AUC Ratio is too low when using only: Reversible IC_{50} values for 3A4 and P-gp only

- **Assumptions:**
  - Perfusion-limited midazolam
  - Permeability-limited liver and kidney for 1-OH-midazolam
  - Ketoconazole: 3A4 total Rev. IC_{50} = 26 nM, ~~3A4 total Irrev. IC_{50} = 15 nM, Kinact = 0.001 min^{-1}~~ and P-gp total IC_{50} = 5.6 µM
  - Reduced fu_{ent} = 4.4% (Ref. Trevaskis-PharmRes-28-9-2176-2011)
- **Clearance:**
  - Paine-J. Pharmacol. Exp. Ther., 283:1552 (1997) unbound K_m = 3.7 µM and V_{max} = 0.977 nmol/min/mg micro. Prot. The 1.15-fold higher clearance was used due to the Olkkola population of 7 females and 2 male subjects.
- **Distribution:**
  - Midazolam Lukacova default Kp calculation
  - 1-OH-midazolam reduced log P = 2.2 to calc. Kps and then ran simulation with log P = 2.57

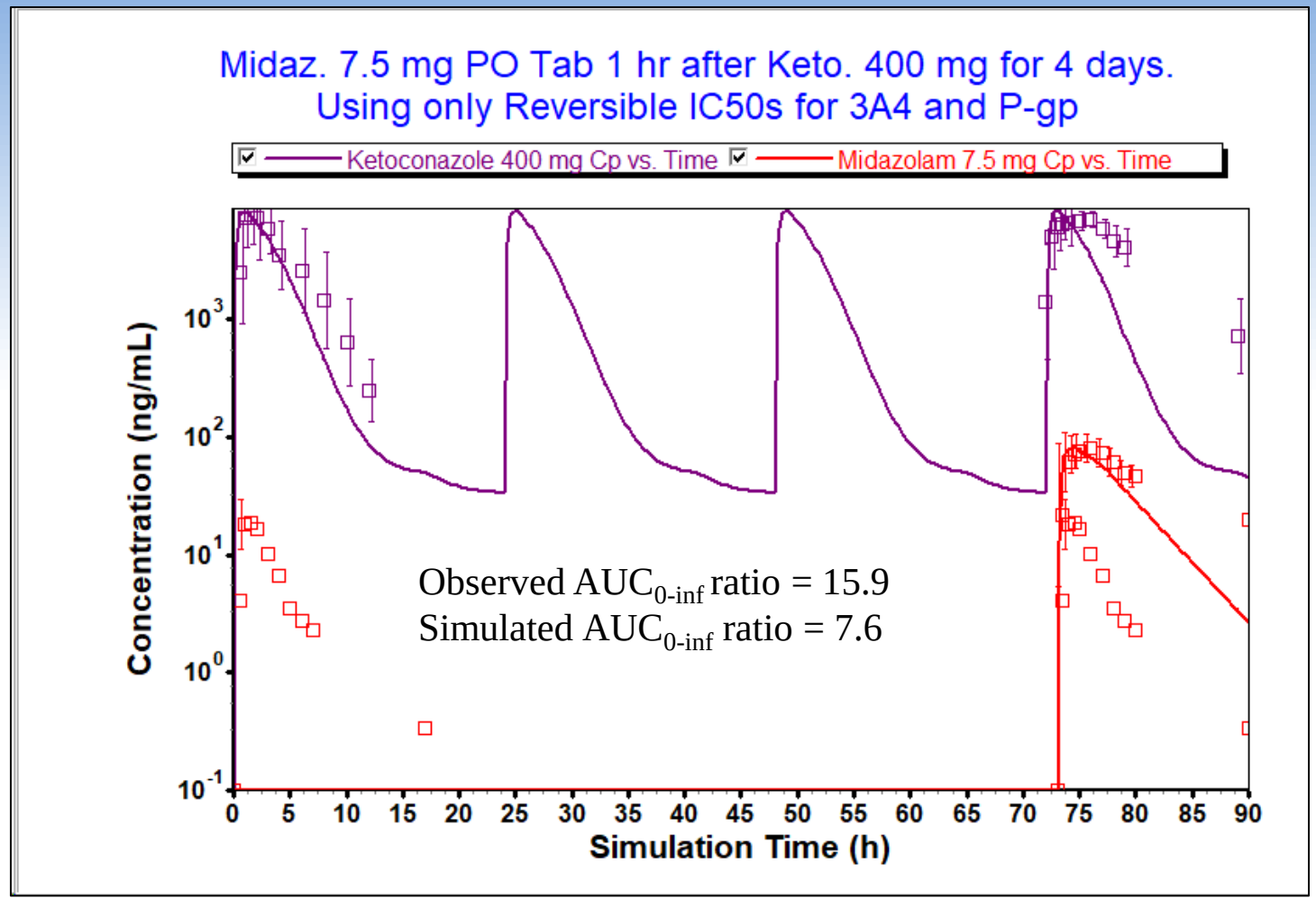

Midazolam clinical data from: Olkkola-ClinPharmacolTherap-55-5-481-1994
Ketoconazole clinical data from: Daneshmend-Antimicrobial agents and Chemotherapy-25-1-1-1984 and Olkkola-ClinPharmacolTherap-55-5-481-1994
Ketoconazole TDI parameters from: Haarhoff-Xenobiotica-47-6-470-2017

In vitro CYP3A Inhibition Parameters ($IC_{50,t,HLM}$) for Ketoconazole

Table 2. Evaluation of CYP3A inhibition with HLM and CLM.

	HLM			CLM		
	IC_{50} (μM)			IC_{50} (μM)		
Inhibitor	Non-preincubation (0 min)	Preincubation (30 min)	Ratio	Non-preincubation (0 min)	Preincubation (30 min)	Ratio
Amprenavir	0.55 ± 0.08	0.084 ± 0.025	6.5	0.3 ± 0.04	0.2 ± 0.03	1.7
Azithromycin	>100	>100	1.0	>100	>100	1.0
Bergamottin	>50	0.17 ± 0.04	>294.1	>50	1.3 ± 0.4	>38.5
Buspirone	>50	15.8 ± 2.9	>3.2	>50	>50	1.0
Cimetidine	>100	>100	1.0	>100	>100	1.0
Clarithromycin	>50	8.2 ± 0.3	>6.1	>50	15.1 ± 0.4	>3.3
Clozapine	>50	21.2 ± 3.7	>2.4	>50	27.2 ± 6.2	>1.8
Cyclosporin A	24.4 ± 5.8	5.8 ± 1.0	4.2	12.0 ± 2.6	7.0 ± 1.5	1.7
Dextromethorphan	>50	>50	1.0	>50	>50	1.0
Diltiazem	43.5 ± 8.6	7.7 ± 1.7	5.6	30.7 ± 4.8	1.4 ± 0.4	21.9
Erythromycin	>100	12.1 ± 3.3	>8.3	>100	54.2 ± 10.2	>1.8
Ethynylestradiol	41.7 ± 1.7	5.2 ± 0.5	8.0	31.4 ± 1.6	4.5 ± 0.8	7.0
Felodipine	4.1 ± 1.3	4.0 ± 0.4	1.0	4.5 ± 1.1	7.4 ± 2.2	0.6
Fluconazole	3.2 ± 0.6	3.7 ± 0.7	0.86	6.8 ± 0.9	6.9 ± 0.6	1.0
Fluoxetine	>50	>50	1.0	>50	>50	1.0
Fluvoxamine	>50	>50	1.0	>50	>50	1.0
Furafylline	>50	>50	1.0	>50	>50	1.0
Irinotecan	>100	>100	1.0	>100	>100	1.0
Isoniazid	>100	>100	1.0	>100	>100	1.0
Itraconazole	0.068 ± 0.017	0.017 ± 0.006	4.0	0.12 ± 0.02	0.054 ± 0.009	2.2
Ketoconazole	0.026 ± 0.010	0.015 ± 0.003	1.7	0.04 ± 0.006	0.056 ± 0.009	0.7
Mibefradil	0.67 ± 0.14	0.017 ± 0.004	39.4	1.0 ± 0.2	0.17 ± 0.04	5.9

- Optimized K_{inact} = 0.001 min^{-1} was used for irreversible inhibition

Publication supporting competitive and time-dependent inhibition by ketoconazole

Haarhoff-Xenobiotica-47-6-470-2017

Midaz. 7.5 mg PO Tab DDI vs. Keto. 400 mg QD for 4 days: Olkkola

Simulated AUC Ratio w/autoinhibition is accurate by adding: Irreversible IC_{50} for 3A4

- **Assumptions:**
  - Perfusion-limited midazolam
  - Permeability-limited liver and kidney for 1-OH-midazolam
  - Ketoconazole: 3A4 total Rev. IC_{50} = 26 nM, 3A4 total Irrev. IC_{50} = 15 nM, Kinact = 0.001 min^{-1} and P-gp total IC_{50} = 5.6 µM
  - Reduced fu_{ent} = 4.4% (Ref. Trevaskis-PharmRes-28-9-2176-2011)
- **Clearance:**
  - Paine-J. Pharmacol. Exp. Ther., 283:1552 (1997) unbound K_m = 3.7 µM and V_{max} = 0.977 nmol/min/mg micro. Prot. The 1.15-fold higher clearance was used due to the Olkkola population of 7 females and 2 male subjects.
- **Distribution:**
  - Midazolam Lukacova default Kp calculation
  - 1-OH-midazolam reduced log P = 2.2 to calc. Kps and then ran simulation with log P = 2.57

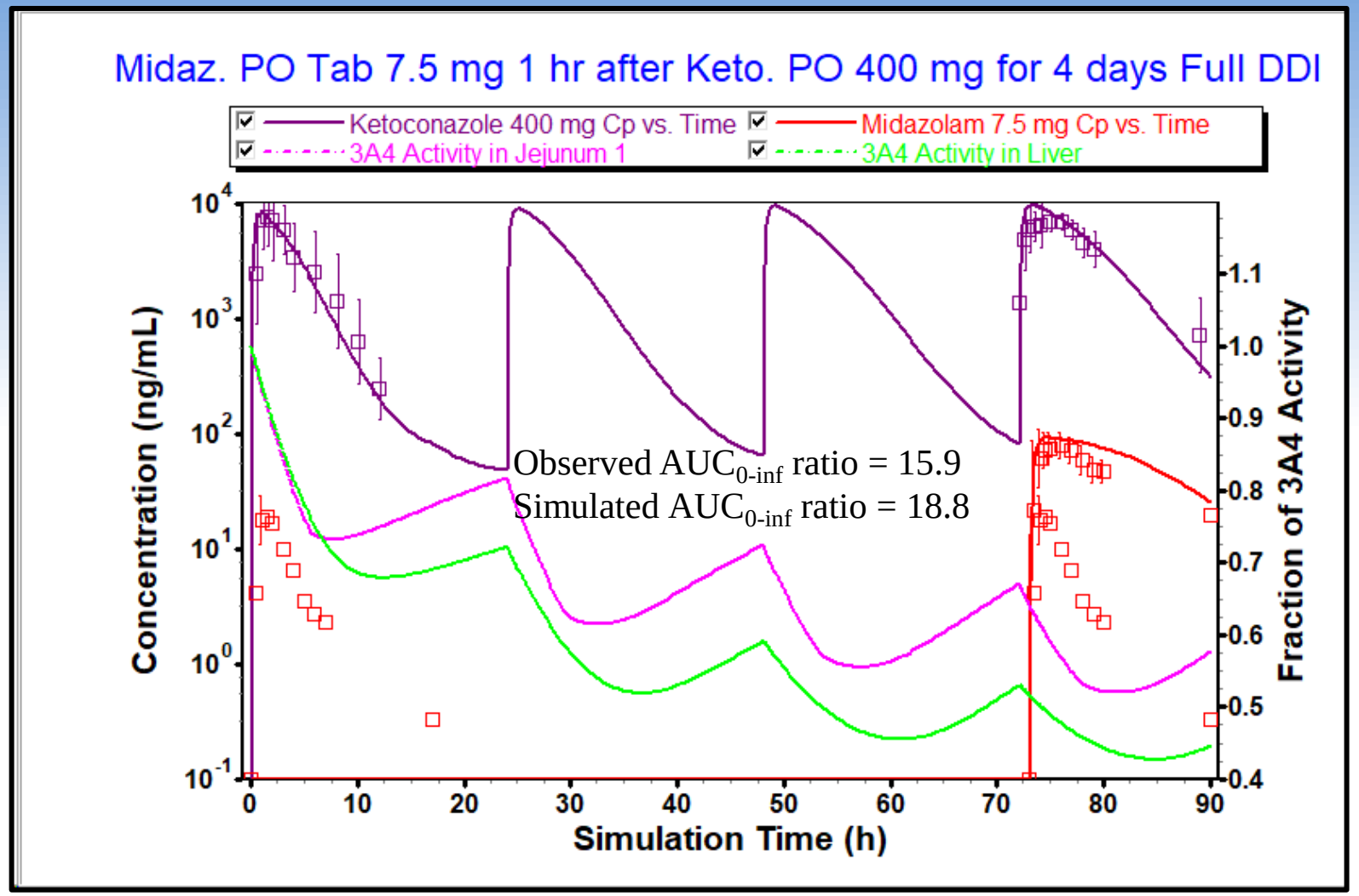

Midazolam clinical data from: Olkkola-ClinPharmacolTherap-55-5-481-1994
Ketoconazole clinical data from: Daneshmend-Antimicrobial agents and Chemotherapy-25-1-1-1984 and Olkkola-ClinPharmacolTherap-55-5-481-1994
Ketoconazole TDI parameters from: Haarhoff-Xenobiotica-47-6-470-2017

Outline of Process for Model Development and Documentation

- Creation of GP a project starts with structure import using ADMET Predictor Module for both substrates and perpetrators.
  - Physicochemical, biopharmaceutical, and biochemical properties
  - Initial evaluation via “Chemistry Classification” with all aspects of ADMET
    - Solubility vs. pH, dissolution, absorption (w/ influx and efflux transporters), clearance (metabolic, biliary, and renal), distribution, excretion, and toxicity.
  - Extensive literature collection and spreadsheet documentation.
    - Workbook with multiple sheets for Physicochemical, Metabolic, Transporter, Preclinical, and Clinical single compound and DDI study data for multiple perpetration mechanisms.
  - First simulations for “Measured Properties” with parameter sensitivity analysis.
  - Model building for individual substrate and/or perpetrator simulations compared to observed data for single escalating doses (for nonlinear dose dependence), multiple dosing (for autoinhibition / autoinduction).
  - DDI simulations for all appropriate mechanisms on both substrate and perpetrator.
  - Analysis of results using the “Guest”* criterion for different levels of accuracy cutoff for increasing AUC (inhibition) and decreasing AUC (induction).
  - Preparation of slides and written reports suitable for regulatory submission.

Newer DDI Module with “Validated” Field

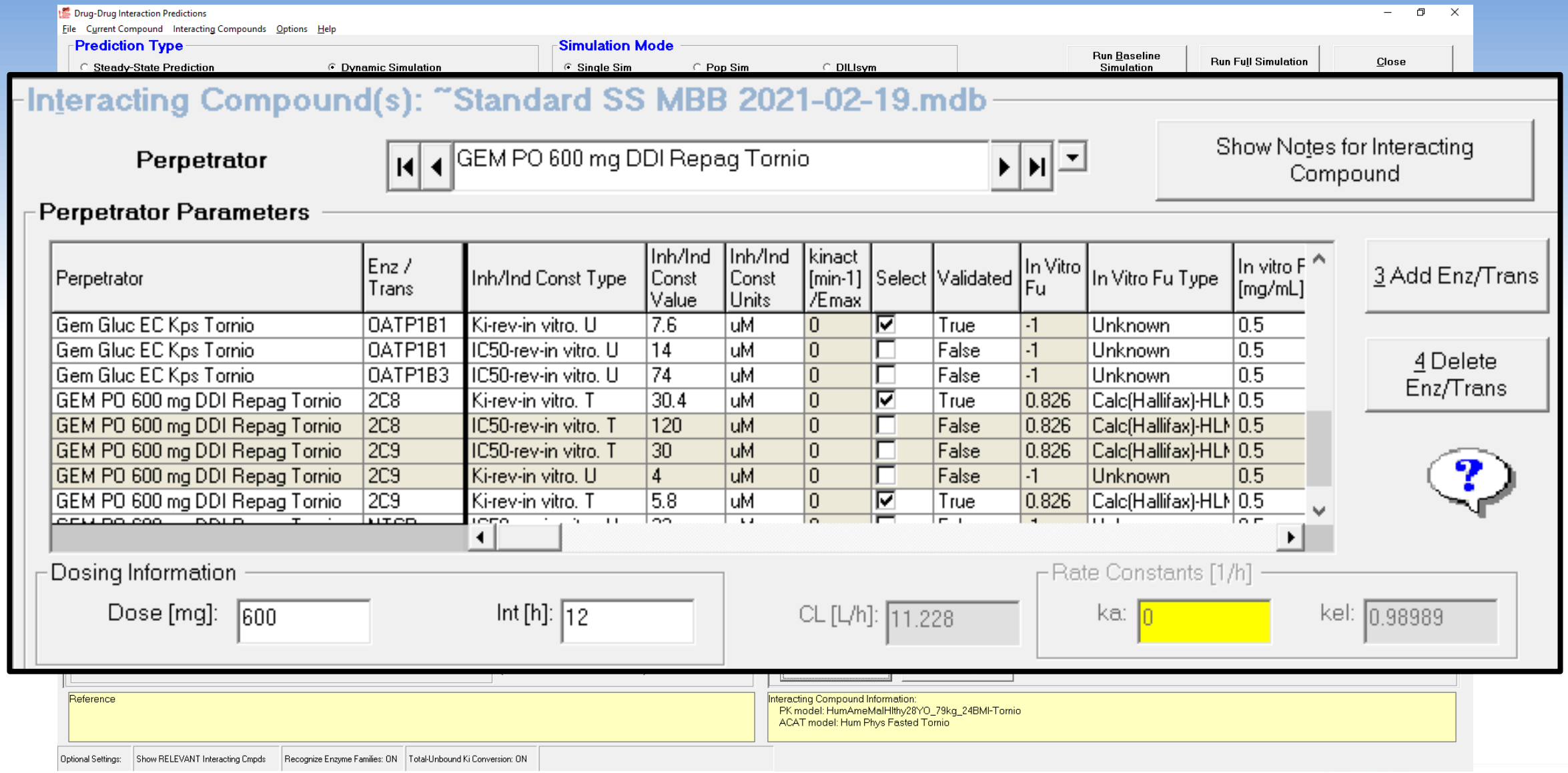

Perpetrator	Enz / Trans	Inh/Ind Const Type	Inh/Ind Const Value	Inh/Ind Const Units	kinact [min-1] /Emax	Select	Validated	In Vitro Fu	In Vitro Fu Type	In vitro F [mg/mL]
Gem Gluc EC Kps Tornio	OATP1B1	Ki-rev-in vitro. U	7.6	uM	0	☑	True	-1	Unknown	0.5
Gem Gluc EC Kps Tornio	OATP1B1	IC50-rev-in vitro. U	14	uM	0	☐	False	-1	Unknown	0.5
Gem Gluc EC Kps Tornio	OATP1B3	IC50-rev-in vitro. U	74	uM	0	☐	False	-1	Unknown	0.5
GEM PO 600 mg DDI Repag Tornio	2C8	Ki-rev-in vitro. T	30.4	uM	0	☑	True	0.826	Calc(Hallifax)-HLM	0.5
GEM PO 600 mg DDI Repag Tornio	2C8	IC50-rev-in vitro. T	120	uM	0	☐	False	0.826	Calc(Hallifax)-HLM	0.5
GEM PO 600 mg DDI Repag Tornio	2C9	IC50-rev-in vitro. T	30	uM	0	☐	False	0.826	Calc(Hallifax)-HLM	0.5
GEM PO 600 mg DDI Repag Tornio	2C9	Ki-rev-in vitro. U	4	uM	0	☐	False	-1	Unknown	0.5
GEM PO 600 mg DDI Repag Tornio	2C9	Ki-rev-in vitro. T	5.8	uM	0	☑	True	0.826	Calc(Hallifax)-HLM	0.5

Repaglinide PO 2.5 mg on Day 3 after 5 doses of GEM 600 mg PO

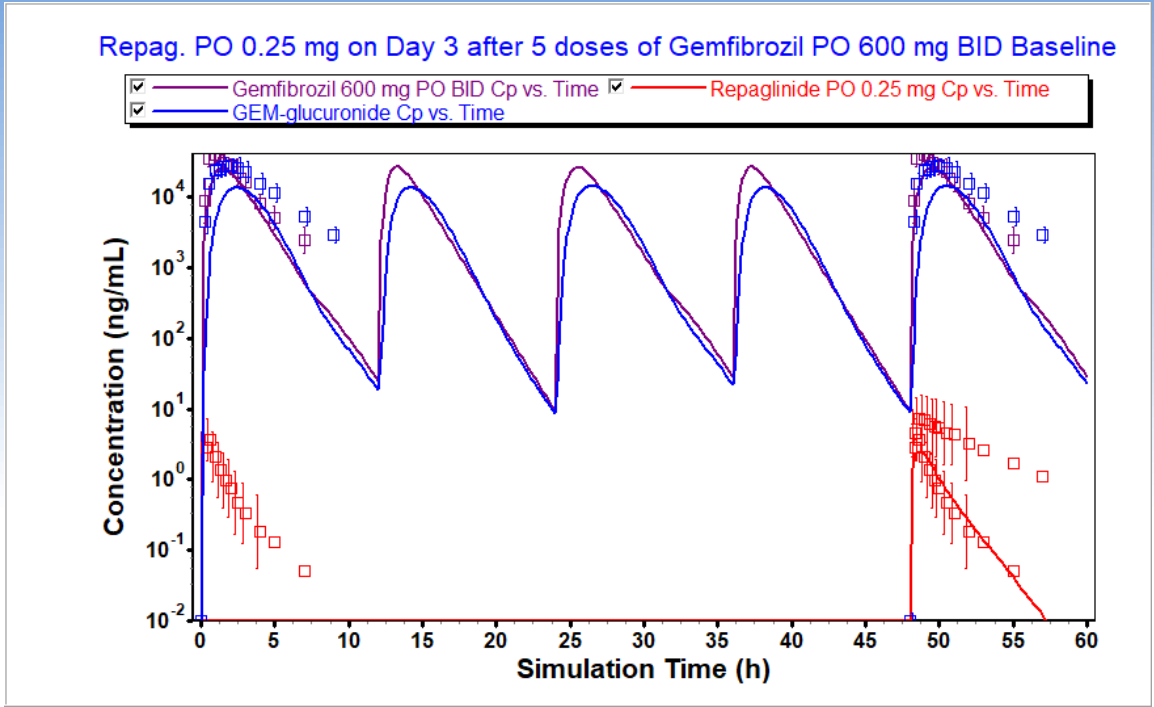

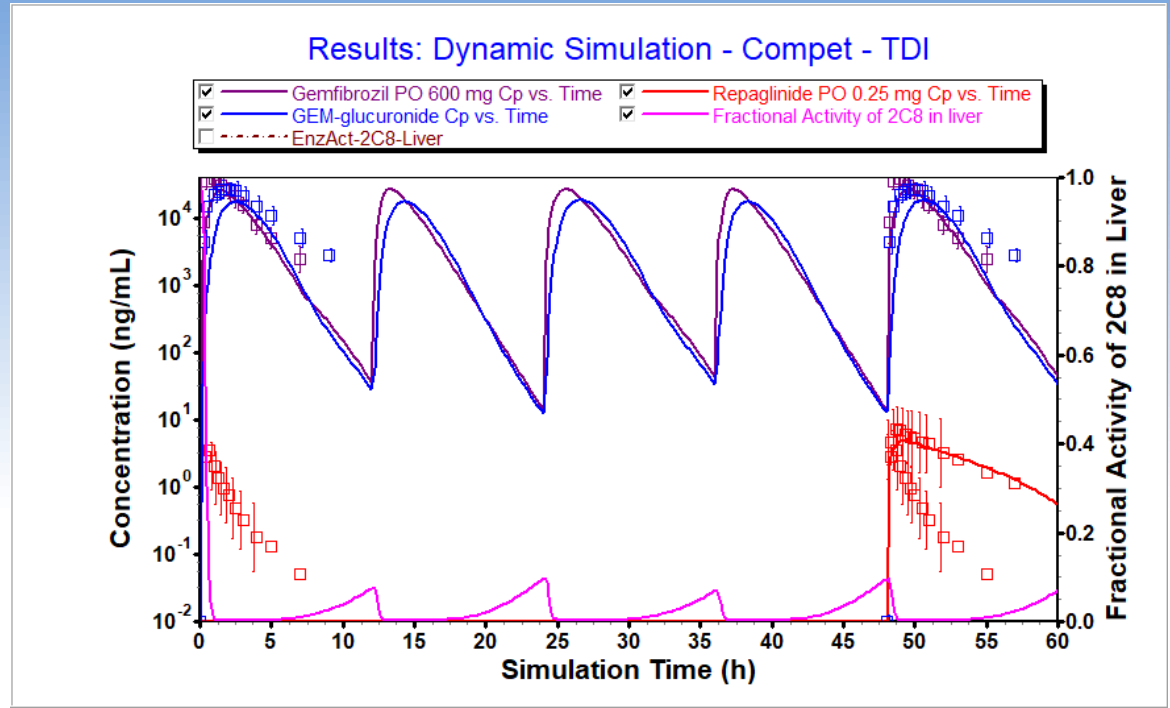

Ki values selected are:
1.) 12.5 uM for OATP1B1 (Gemfibrozil parent)
2.) 7.6 uM for OATP1B1 (Glucuronide)
3.) 30.4 uM for the CYP2C8 (Reversible) for the parent and
4.) 20 uM for Irrev inhibition and Kinact= 0.21 min^{-1} of CYP2C8 for the Glucuronide
5.) 3.4 uM for the OAT3 (Rev inhibition) for the parent and
6.) 9.9 uM for the OAT3 (Rev inhibition) Glucuronide
7.) 5.8 uM for the CYP2C9 (Rev Inhibition) by Parent

Repaglinide record: Repaglinide_PO_0.25mg_Gem 600 mg
GEM Record:GEM PO 600 mg DDI Repag Tornio
GEM-Gluc record: Gem-Gluc EC Kps Tornio
Gemfibrozil was dosed with DDI module (600 mg, BID dosing interval)
Observed data for GEM and GEM gluc and Repaglinide before and after DDI in the plot is from Tornio et. al., 2008

Tornio et. al., Clin. Pharmacol. Thera. 84(3):403(2008)

Outline of Process for Model Development and Documentation

- Creation of GP a project starts with structure import using ADMET Predictor Module for both substrates and perpetrators.
  - Physicochemical, biopharmaceutical, and biochemical properties
  - Initial evaluation via “Chemistry Classification” with all aspects of ADMET
    - Solubility vs. pH, dissolution, absorption (w/ influx and efflux transporters), clearance (metabolic, biliary, and renal), distribution, excretion, and toxicity.
  - Extensive literature collection and spreadsheet documentation.
    - Workbook with multiple sheets for Physicochemical, Metabolic, Transporter, Preclinical, and Clinical single compound and DDI study data for multiple perpetration mechanisms.
  - First simulations for “Measured Properties” with parameter sensitivity analysis.
  - Model building for individual substrate and/or perpetrator simulations compared to observed data for single escalating doses (for nonlinear dose dependence), multiple dosing (for autoinhibition / autoinduction).
  - DDI simulations for all appropriate mechanisms on both substrate and perpetrator.
  - Analysis of results using the “Guest”* criterion for different levels of accuracy cutoff for increasing AUC (inhibition) and decreasing AUC (induction).
  - Preparation of slides and written reports suitable for regulatory submission.

Eleanor J. Guest et al. DMD, 39(2):170 (2011)

Materials and Methods

The traditional two-fold predictive measure is bounded two-fold above and below the observed value: any prediction within these boundaries is classed as a successful prediction (see Fig. 1). Therefore, if the observed ratio, $AUC_{+inhibitor}/AUC_{control}$, is 1, the boundaries would be from 0.5 to 2.0. As noted in the *Introduction*, this range is too wide for an interaction, which is in fact not present. As a result, we propose new limits, as shown in eqs. 1 to 3 below. The limits coalesce when the observed ratio is 1 and approach the traditional two-fold limits as the ratio becomes larger (Fig. 1).

$$\text{Upper limit: } R_{obs} * \text{Limit} \quad (1)$$

Lower limit: R_o

$$\text{Limit} = \frac{1 + 2(R}{R_}$$

where R_{obs} represents $AUC_{+inhibitor}/AUC$ inhibition DDIs. The new predictive measu

fold. The trend of lower prediction accuracy at higher potency of DDIs reported in previous studies is no longer apparent when predictions are assessed via the new predictive measure. Thus, the study proposes a more logical method for the assessment of prediction success and its application for induction and inhibition DDIs.

To allow for uncertainty in the observed [illegible], the impact of variability was assessed by considering DDIs involving midazolam; a commonly used CYP3A4 victim drug (Bjornsson et al., 2003; Galetin et al., 2005). In this case, upper and lower limits are as defined in eqs. 1 and 2, respectively, but the variability is now introduced into the limit as shown in eq. 4.

$$\text{Limit} = \frac{\delta + 2(R_{obs} - 1)}{R_{obs}} \quad (4)$$

where δ is a parameter that accounts for variability. If $\delta = 1$, there is no variability and limits revert to those defined by eq. 3. If $\delta = 1.25$ and $R_{obs} = 1$, then the limits on R are between 0.80 and 1.25, corresponding to the conventional 20% limits used in bioequivalence testing (United States Food and Drug Administration, 2003). Note that these limits are symmetrical on the

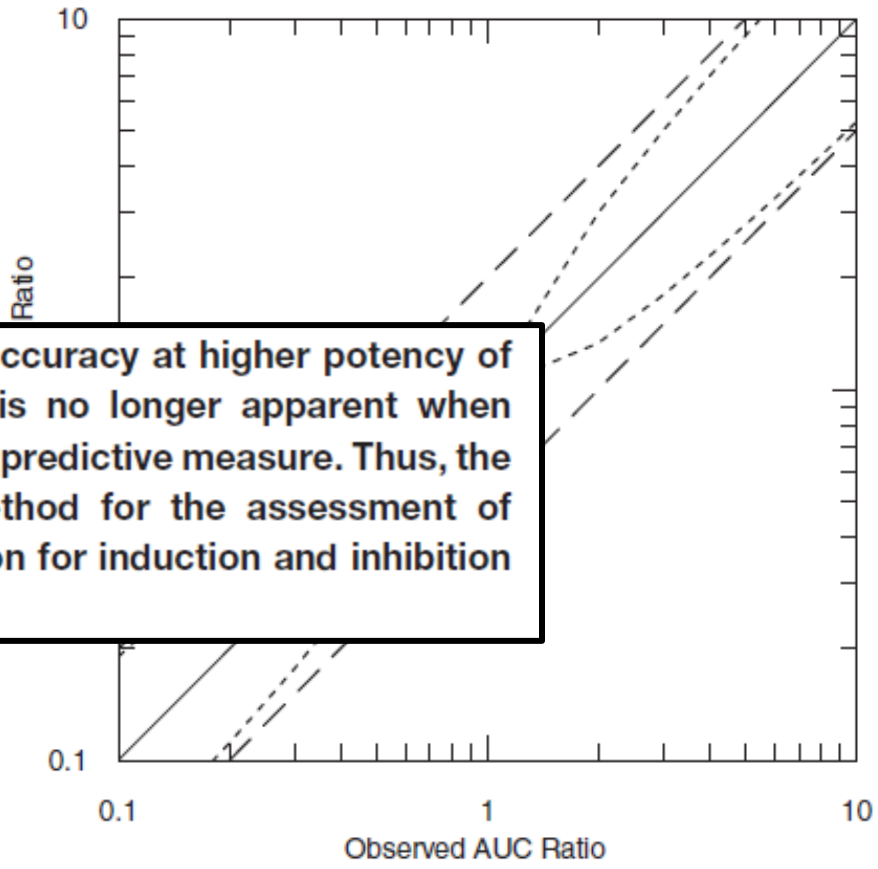

FIG. 1. Schematic graph displaying the limits of the different predictive measures; the traditional two-fold predictive measure (dashed lines) and the proposed new predictive measure (dotted lines). Observed AUC ratios include both induction and inhibition DDIs.

Repag. PO 0.25 mg on Day 3 after GEM PO 600 mg BID

GastroPlus(TM) 9.8.1003	2/23/2021	11:56:12 PM					
Compound 1:	Victim						
Database:	Repaglinide-GP9.8-DDI-Standard-2021-01-13.mdb						
Record:	Repag PO 0.25mg DDI Gem 600mg-Tornio2008						
Compound 2:	**Perpetrator: Gemfibrozil 600 mg PO BID for 5 doses**						
Database:	Gemfibrozil GP9.8.1003 DDI Standard SS MBB 2021-02-19.mdb						
Record:	GEM PO 600 mg DDI Repag Tornio						
[NewTable]	Dynamic Simulation Results						
Compound	Fa [%]	FDp [%]	F [%]	Cmax [ug/mL]	Tmax [h]	AUC(0-t) [ng-h/mL]	AUC(0-inf) [ng-h/mL]
Repag PO 0.25mg DDI Gem 600mg-Tornio2008-baseline	100	80.74	51.87	0.00239	48.6	5.076	5.079
GEM PO 600 mg DDI Repag Tornio-baseline	109.1	106.7	96.15	27.08	37.3	348000	348000
Gem Gluc EC Kps Tornio-baseline	0	0	0	14.57	50.5	229000	229000
Repag PO 0.25mg DDI Gem 600mg-Tornio2008-DDI	100	80.63	72.99	0.00512	49.2	29.47	31.12
GEM PO 600 mg DDI Repag Tornio-DDI	109.1	106.7	96.74	27.98	37.3	397000	397000
Gem Gluc EC Kps Tornio-DDI	0	0	0	19.25	50.6	310000	310000
Repag PO 0.25mg DDI Gem 600mg-Tornio2008-ratio	1	0.999	1.407	2.142	1.012	5.806	6.127
GEM PO 600 mg DDI Repag Tornio-ratio	1	1	1.006	1.033	1	1.141	1.141
Gem Gluc EC Kps Tornio-ratio	0	0	0	1.321	1.002	1.354	1.354

Table 1 Pharmacokinetics of repaglinide after a single oral dose of 0.25 mg repaglinide in 10 healthy volunteers, after pretreatment with 600 mg gemfibrozil twice daily, when repaglinide was administered 0, 3, 6, or 12 h after the last gemfibrozil dose

		Time from the last gemfibrozil dose			
Variable	Control	0 h	3 h	6 h	12 h
Repaglinide					
C_{max} (ng/ml)	3.7 ± 2.7	8.1 ± 3.2***	7.2 ± 2.3***	8.3 ± 2.8***,‡	8.1 ± 2.4***,‡
Fold (range)		2.2 (1.4–2.9)	1.9 (1.1–2.9)	2.2 (1.1–3.4)	2.2 (1.2–3.3)
$t_{½}$ (h)	1.2 ± 0.2	3.0 ± 0.4***	2.7 ± 0.3***,†	2.4 ± 0.2***,†	2.0 ± 0.3***,†††,‡‡,¶¶
Fold (range)		2.6 (1.9–4.3)	2.3 (1.7–3.7)	2.1 (1.6–3.3)	1.7 (1.5–2.6)
AUC_{0-9h} (ng·h/ml)	4.8 ± 4.3	29.3 ± 7.7***	27.8 ± 9.4***	27.5 ± 8.6***	22.9 ± 7.4***,††,‡
Fold (range)		6.1 (2.6–12)	5.8 (2.5–13)	5.7 (2.5–9.2)	4.7 (2.1–7.8)
$AUC_{0-\infty}$ (ng·h/ml)	4.9 ± 4.4	34.2 ± 9.3***	31.5 ± 11.2***	30.2 ± 9.3***	24.5 ± 8.2***,††,‡,¶¶¶
Fold (range)		7.0 (2.9–14)	6.5 (2.8–15)	6.2 (2.7–10)	5.0 (2.2–8.5)

	Observed	Simulated
Cmax Ratio	2.2	2.1
AUC(0-t) Ratio	6.1	5.8

	Cmax	AUC(0-t)
Guest Method Limit	1.66	1.88
Upper Limit	3.65	11.45
Lower Limit	1.33	3.25

Observed DDI ratio for Repaglinide AUC_{0-t} = 6.1

Predicted DDI ratio for Repaglinide AUC_{0-t} = 5.8

Midazolam DDI vs. Fluconazole

		Variability	1.25	Guest Limits					log Limits		
	Obs Ratio	Variability (CV)	Limit	Upper	Lower	Unity	2-fold(+)	2-fold(-)	UL	LL	Center
Reciprocal of ratio 2 -10	0.10	1.25	1.93	0.19	0.05	0.10	0.20	0.05	-0.28	0.28	0
	0.13	1.25	1.91	0.24	0.07	0.13	0.25	0.06	-0.28	0.28	0
	0.25	1.25	1.81	0.45	0.14	0.25	0.50	0.13	-0.26	0.26	0
	0.33	1.25	1.75	0.58	0.19	0.33	0.67	0.17	-0.24	0.24	0
	0.50	1.25	1.63	0.81	0.31	0.50	1.00	0.25	-0.21	0.21	0.00
	1.00	1.25	1.25	1.25	0.80	1	2.00	0.50	0.10	-0.10	0
	2.00	1.25	1.63	3.25	1.23	2	4.00	1.00	0.21	-0.21	0
	3.00	1.25	1.75	5.25	1.71	3	6.00	1.50	0.24	-0.24	0
	4.00	1.25	1.81	7.25	2.21	4	8.00	2.00	0.26	-0.26	0
	8.00	1.25	1.91	15.25	4.20	8	16.00	4.00	0.28	-0.28	0
	10.00	1.25	1.93	19.25	5.19	10	20.00	5.00	0.28	-0.28	0

Guest Criteria for Ki = 15 uM					Guest Criteria for Ki = 15 uM				
CV	Limit	Up Lim	Low Lim	Predicted	CV	Limit	Up Lim	Low Lim	Predicted
Cmax					AUC0-t				
1.25	1.67	3.84	1.37	2.07	1.25	1.80	6.70	2.07	3.69
1.25	1.58	2.82	1.13	1.86	1.25	1.78	6.13	1.93	3.23
1.25	-	-	-	-	1.25	1.57	2.73	1.11	1.79

Guest Criteria for Ki = 7.4 uM					Guest Criteria for Ki = 7.4 uM				
CV	Limit	Up Lim	Low Lim	Predicted	CV	Limit	Up Lim	Low Lim	Predicted
Cmax					AUC0-t				
1.25	1.67	3.84	1.37	2.57	1.25	1.80	6.70	2.07	6.19
1.25	1.58	2.82	1.13	2.32	1.25	1.78	6.13	1.93	5.50
1.25	-	-	-	-	1.25	1.57	2.73	1.11	2.37

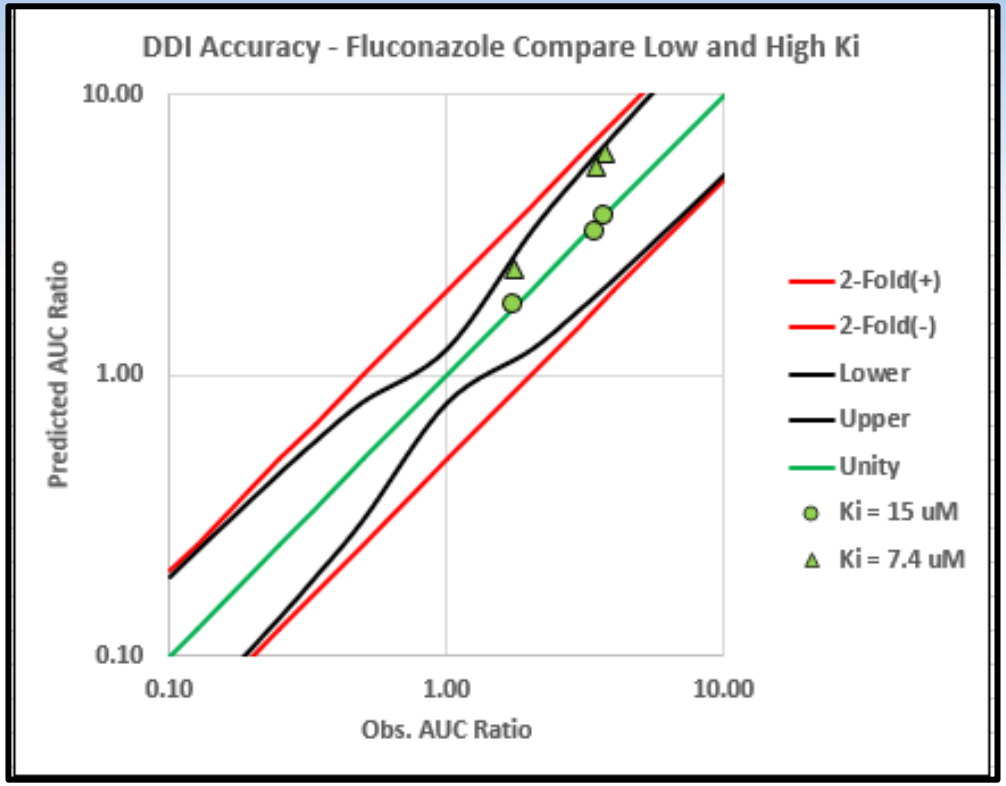

SimulationsPlus
SCIENCE + SOFTWARE = SUCCESS

Using Guest Plot to Optimize Rifampicin Induction Parameters for GP9.8.1

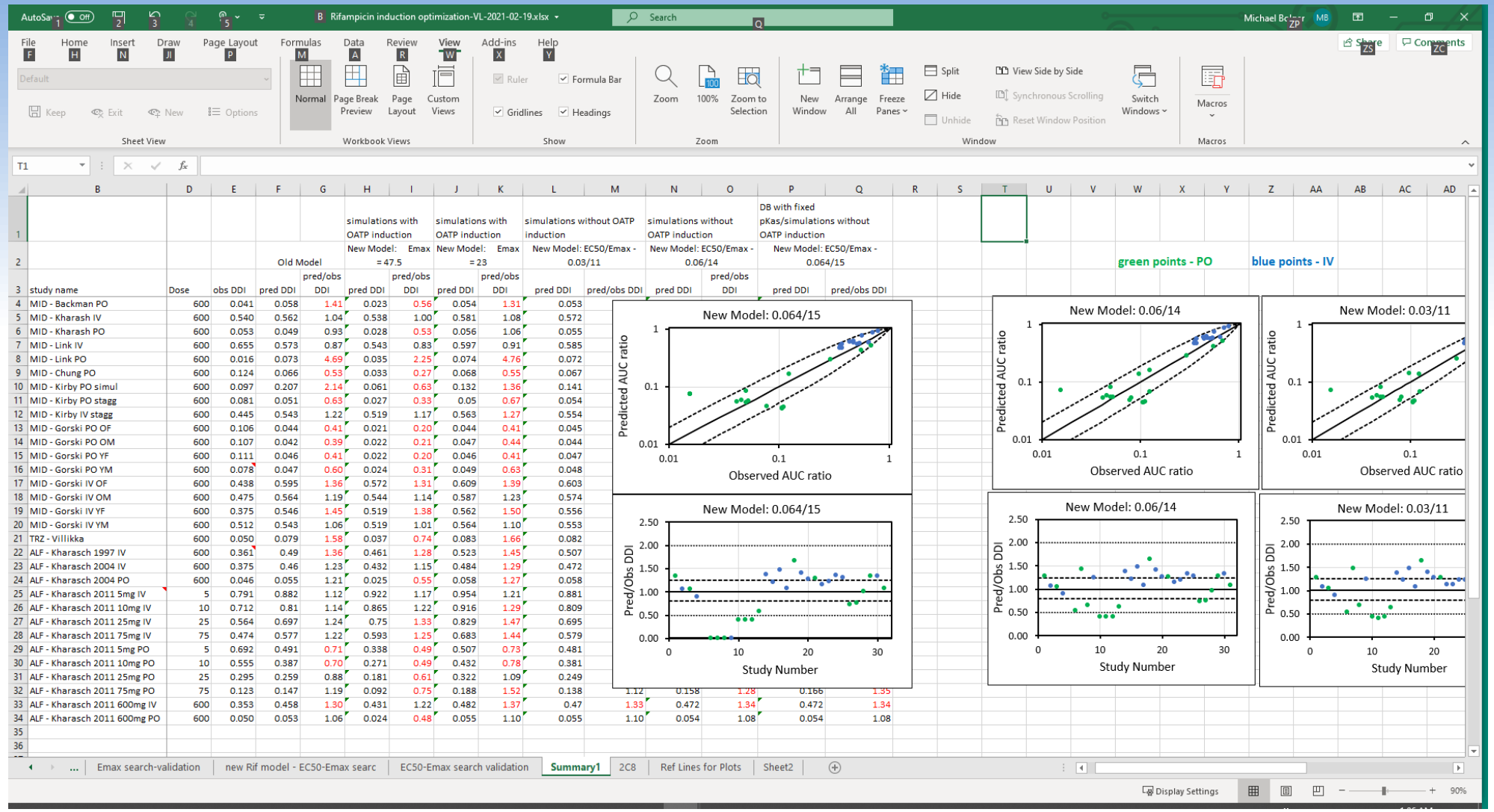

study name	Dose	obs DDI	old model pred DDI	old model pred/obs DDI	Emax 47.5 pred DDI	Emax 47.5 pred/obs DDI	Emax 23 pred DDI	Emax 23 pred/obs DDI	EC50/Emax 0.03/11 pred DDI	EC50/Emax 0.03/11 pred/obs DDI	EC50/Emax 0.06/14 pred DDI	EC50/Emax 0.06/14 pred/obs DDI	EC50/Emax 0.064/15 pred DDI	EC50/Emax 0.064/15 pred/obs DDI
MID - Backman PO	600	0.041	0.058	1.41	0.023	0.56	0.054	1.31	0.053					
MID - Kharash IV	600	0.540	0.562	1.04	0.538	1.00	0.581	1.08	0.572					
MID - Kharash PO	600	0.053	0.049	0.93	0.028	0.53	0.056	1.06	0.055					
MID - Link IV	600	0.655	0.573	0.87	0.543	0.83	0.597	0.91	0.585					
MID - Link PO	600	0.016	0.073	4.69	0.035	2.25	0.074	4.76	0.072					
MID - Chung PO	600	0.124	0.066	0.53	0.033	0.27	0.068	0.55	0.067					
MID - Kirby PO simul	600	0.097	0.207	2.14	0.061	0.63	0.132	1.36	0.141					
MID - Kirby PO stagg	600	0.081	0.051	0.63	0.027	0.33	0.05	0.67	0.054					
MID - Kirby IV stagg	600	0.445	0.543	1.22	0.519	1.17	0.563	1.27	0.554					
MID - Gorski PO OF	600	0.106	0.044	0.41	0.021	0.20	0.044	0.41	0.045					
MID - Gorski PO OM	600	0.107	0.042	0.39	0.022	0.21	0.047	0.44	0.044					
MID - Gorski PO YF	600	0.111	0.046	0.41	0.022	0.20	0.046	0.41	0.047					
MID - Gorski PO YM	600	0.078	0.047	0.60	0.024	0.31	0.049	0.63	0.048					
MID - Gorski IV OF	600	0.438	0.595	1.36	0.572	1.31	0.609	1.39	0.603					
MID - Gorski IV OM	600	0.475	0.564	1.19	0.544	1.14	0.587	1.23	0.574					
MID - Gorski IV YF	600	0.375	0.546	1.45	0.519	1.38	0.562	1.50	0.556					
MID - Gorski IV YM	600	0.512	0.543	1.06	0.519	1.01	0.564	1.10	0.553					
TRZ - Villikka	600	0.050	0.079	1.58	0.037	0.74	0.083	1.66	0.082					
ALF - Kharasch 1997 IV	600	0.361	0.49	1.36	0.461	1.28	0.523	1.45	0.507					
ALF - Kharasch 2004 IV	600	0.375	0.46	1.23	0.432	1.15	0.484	1.29	0.472					
ALF - Kharasch 2004 PO	600	0.046	0.055	1.21	0.025	0.55	0.058	1.27	0.058					
ALF - Kharasch 2011 5mg IV	5	0.791	0.882	1.12	0.922	1.17	0.954	1.21	0.881					
ALF - Kharasch 2011 10mg IV	10	0.712	0.81	1.14	0.865	1.22	0.916	1.29	0.809					
ALF - Kharasch 2011 25mg IV	25	0.564	0.697	1.24	0.75	1.33	0.829	1.47	0.695					
ALF - Kharasch 2011 75mg IV	75	0.474	0.577	1.22	0.593	1.25	0.683	1.44	0.579					
ALF - Kharasch 2011 5mg PO	5	0.692	0.491	0.71	0.338	0.49	0.507	0.73	0.481					
ALF - Kharasch 2011 10mg PO	10	0.555	0.387	0.70	0.271	0.49	0.432	0.78	0.381					
ALF - Kharasch 2011 25mg PO	25	0.295	0.259	0.88	0.181	0.61	0.322	1.09	0.249					
ALF - Kharasch 2011 75mg PO	75	0.123	0.147	1.19	0.092	0.75	0.188	1.52	0.138	1.12	0.158	1.28	0.166	1.35
ALF - Kharasch 2011 600mg IV	600	0.353	0.458	1.30	0.431	1.22	0.482	1.37	0.47	1.33	0.472	1.34	0.472	1.34
ALF - Kharasch 2011 600mg PO	600	0.050	0.053	1.06	0.024	0.48	0.055	1.10	0.055	1.10	0.054	1.08	0.054	1.08

Outline of Process for Model Development and Documentation

- Creation of GP a project starts with structure import using ADMET Predictor Module for both substrates and perpetrators.
  - Physicochemical, biopharmaceutical, and biochemical properties
  - Initial evaluation via “Chemistry Classification” with all aspects of ADMET
    - Solubility vs. pH, dissolution, absorption (w/ influx and efflux transporters), clearance (metabolic, biliary, and renal), distribution, excretion, and toxicity.
  - Extensive literature collection and spreadsheet documentation.
    - Workbook with multiple sheets for Physicochemical, Metabolic, Transporter, Preclinical, and Clinical single compound and DDI study data for multiple perpetration mechanisms.
  - First simulations for “Measured Properties” with parameter sensitivity analysis.
  - Model building for individual substrate and/or perpetrator simulations compared to observed data for single escalating doses (for nonlinear dose dependence), multiple dosing (for autoinhibition / autoinduction).
  - DDI simulations for all appropriate mechanisms on both substrate and perpetrator.
  - Analysis of results using the “Guest”* criterion for different levels of accuracy cutoff for increasing AUC (inhibition) and decreasing AUC (induction).
  - Preparation of slides and written reports suitable for regulatory submission.

Written Report of Model Development and Validations

Development of a Whole-Body Physiologically Based Pharmacokinetic Model of Rifampicin and Model Validation with Known Drug-Drug Interactions (Midazolam, Triazolam, Rosiglitazone, Repaglinide, Voriconazole)

Suvarchala Avvari, Viera Lukacova, Michael B. Bolger

1. Introduction

A whole-body physiologically based pharmacokinetic (PBPK) model of rifampicin (RIF) was developed accounting for the enzymes involved in the auto-induction and metabolism of RIF such as (CYP3A4, CYP2C8, CYP2C9, UGT1A3), active uptake transporter (OATP1B1), and efflux transporter (MRP2) for the prediction of known drug-drug interactions (DDIs) with midazolam (MDZ), triazolam, and rosiglitazone substrates using GastroPlus® version 9.8 (Simulations Plus, Inc.). The model was developed to capture the different *in-vivo* mechanisms involved in the absorption, distribution, metabolism, and elimination of RIF. PBPK models parameterized with *in silico, in vitro,* and *in vivo* data have been extensively used to evaluate the potential for DDIs, arising due to enzyme and/or transporter induction and reversible or irreversible time-dependent inhibition (Zhang et al. 2020). The current report describes a model of RIF built using GastroPlus that includes all the relevant enzyme and transporter related mechanisms for DDI modeling of novel substrates and perpetrators.

2. Model Development (GastroPlus v.9.8) of Rifampicin and Parameter Input Selection

In this study, PBPK models of RIF were built using the *in vitro* data when possible. Plasma concentration-time (C_p-time) profiles of published clinical studies covering the full reported dosing range were used for model development in both healthy subjects and tuberculosis (TB) patients. In some studies, the information regarding the amount of unchanged drug excreted in urine was available and it was utilized to inform the model optimization. All clinical studies used for model development in healthy subjects and TB patients are listed in Table 1 with descriptions pertaining to the study. Simulations were carried out using age, sex, weight, and body mass index (BMI) that matched the corresponding clinical studies. If information regarding the demographics of the study population was not available, a reasonable assumption was made to describe the individual and population physiology of each study.

PBPK MODEL: RIFAMPICIN

Table 1. Clinical PK Data used for RIF PBPK Model Calibration and Qualification

Study Type	Description	Reference
Rifampicin		
Pharmacokinetic (PK) study of intravenous (IV) RIF	The time course of the serum and urine concentrations of RIF were evaluated during and after IV administration of RIF in healthy subjects. Dose levels of 300 mg, 450 mg, and 600 mg as IV infusions (3 hr) in 500 mL of glucose solution.	(Nitti et al. 1977)
Population PK modeling of RIF	Subjects fasted from 10 p.m. before the doses were given until 4 hr afterward. Water was allowed until 2 hr before the doses were administered. On the study day, 2 capsules (each containing 300 mg of RIF) were administered. The C_p-time profiles were measured in twenty-four healthy male subjects.	(Peloquin et al. 1997)
PK of oral (PO) and IV RIF during chronic administration in TB patients.	After overnight fasting, the subjects ingested 600 mg of RIF for either PO or IV infusion (1 hr). The solution for the RIF infusion was prepared by dissolving the content of a 600 mg vial in 10 mL of solvent, which was transferred into 500 mL isotonic saline solution. Both the PO and IV PK of RIF were measured on Days 1-2, Days 8-9, and Days 22-23 in 12 TB subjects.	(Loos et al. 1985)
PK study of RIF	The study was carried out in 18 healthy subjects. RIF was administered as 300 mg capsules and the treatment lasted for 14 days. Three dose levels were investigated: 900 mg and 600 mg in a single dose, and 600 mg divided daily into 2 doses of 300 mg each. The plasma concentrations of RIF were measured on Days 1, 4, 6, and 14.	(Acocella et al. 1971)
DDI studies used for model verification		
DDI study of the effect of RIF PO 600 mg on the PK of MDZ PO (3 mg) and IV (1 mg) in healthy subjects	For the study of hepatic and intestinal CYP3A4 induction, RIF (INN, rifampicin) (600 mg) was administered orally at bedtime for 5 days; 1 mg IV MDZ was then administered, followed 1 hr later by administration of 15 µg/kg IV Alfentanil (ALF), RIF at bedtime, and on the next day 3 mg PO MDZ with 50 mL apple juice, followed 1 hr later by 60 g/kg oral ALF.	(Kharasch et al. 2004)
The effect of RIF treatment on the PK and pharmacodynamics (PD) of MDZ PO (15 mg) in healthy subjects	The subjects were given PO doses of either 600 mg RIF (two 300 mg capsules) or matched placebo once daily at 8 PM for 5 days. On Day 6, a 15 mg tablet of MDZ was ingested with 150 mL water at 1 PM, that is, 17 hrs after	(Backman, Olkkola, and Neuvonen 1996)

Written Report of Model Development and Validations

Table 6 **Baseline Simulations of Sensitive CYP3A4 Substrates: Simulated Versus Observed PK Parameters of Triazolam and Midazolam.**

Reference	Substrate Dose and Regimen	Observed#		Simulated	
		C_{max} (ng/mL)	AUC_{0-t} (ng*hr/mL)	C_{max} (ng/mL)	AUC_{0-t} (ng*hr/mL)
(Varhe, Olkkola et al. 1994)	**0.25 mg single dose triazolam tablet**	1.5 ± 0.2	5.9 ± 0.7	1.49	8.86
(Greenblatt, Wright et al. 1998)	**0.25 mg single dose triazolam tablet**	2.6 ± 0.3	10.6 ± 1.6$	1.82	11.06$
(Olkkola, Backman et al. 1994)	**7.5 mg PO midazolam**	22 ± 6	65± 10$	25	82.99$

#Observed values are from the average of individual values, and represent mean ± standard error; $represent AUC_{0-inf}

Table 7 **DDI Simulations of Sensitive CYP3A4 Substrates: Simulated Versus Observed PK Parameters of Triazolam and Midazolam With or Without Co-administration of Ketoconazole**

Reference	Substrate		C_{max} (ng/mL)	AUC_{0-t} (ng*h/mL)
(Varhe, Olkkola et al. 1994)	**Triazolam**	Observed baseline#	1.5 ± 0.2	5.9 ± 0.7
		Simulated baseline	1.49	8.86
		Observed DDI #	4.6 ± 0.5	48.1 ± 5.3
		Simulated DDI	4.24	55.82
		Observed DDI ratio#	3.07	8.1
		Simulated DDI ratio	2.85	6.3
(Greenblatt, Wright et al. 1998)	**Triazolam**	Observed baseline#	2.6 ± 0.3	10.6 ± 1.6$
		Simulated baseline	1.82	11.06$
		Observed DDI #	5.4 ± 0.4	145.4 ± 39.1$
		Simulated DDI	4.71	142.6$
		Observed DDI ratio#	2.1	13.7$
		Simulated DDI ratio	2.59	12.9$
(Olkkola, Backman et al. 1994)	**Midazolam**	Observed baseline#	22 ± 6$	65 ± 10$
		Simulated baseline	25	82.99$
		Observed DDI#	90 ± 7	1033.3$
		Simulated DDI	96	1300.7$
		Observed DDI ratio	4.09	15.9$
		Simulated DDI ratio	3.84	15.7$

#Parameters are from the average of observed individual values and represent mean ± standard error; $represent AUC_{0-inf}; the simulated DDI ratios were highlighted in green while observed DDI ratios were highlighted in blue.

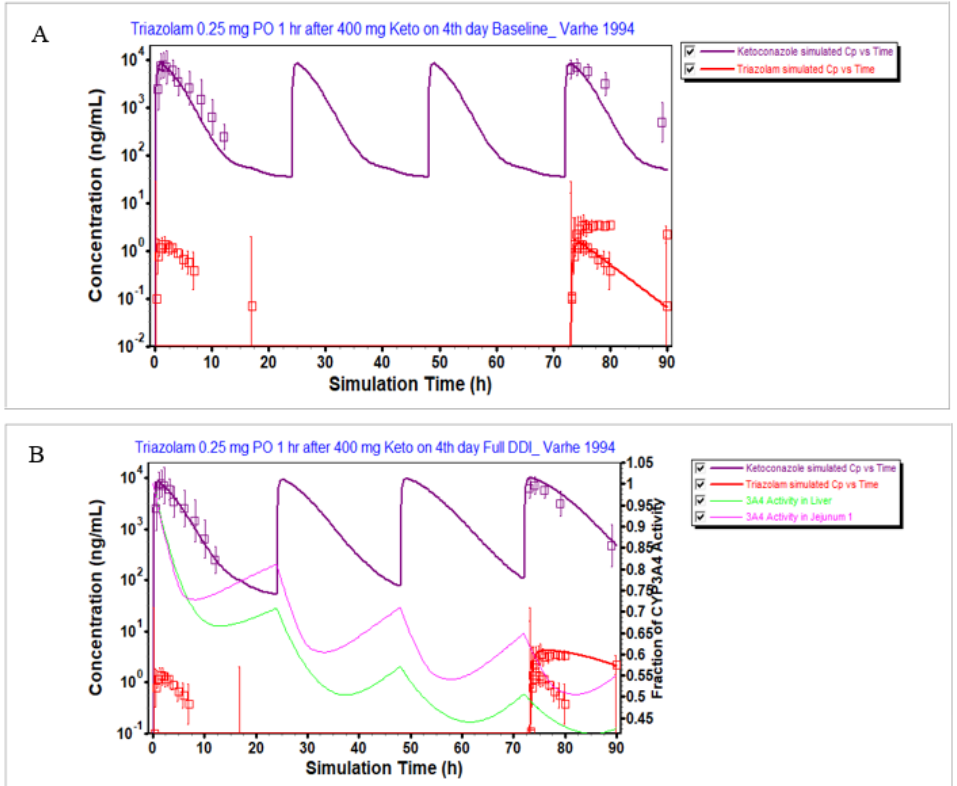

Figure 6 **Baseline Simulation Without a Drug-Drug Interaction (A, Top) and Full Dynamic Simulation With a Drug-Drug Interaction (B, Bottom) Between Ketoconazole and Triazolam**

Ketoconazole (400 mg) was administered for four doses, and 0.25 mg triazolam was given at 3 PM after the fourth dose of KCZ (given at 2 PM) (Varhe, Olkkola et al. 1994).

The open squares and error bars represent the mean observed data and coefficient of variation, respectively, and the simulated (line) C_p-time profiles for triazolam (red) and ketoconazole (purple). The simulated CYP3A4 activity in liver is highlighted in green, and the simulated

Conclusions

- The GP DDI Standard Update Project Team have made significant advances in the ability to simulate complex mechanistic drug-drug interactions involving enzymes, transporters, and enterohepatic circulation.
- Now DDI simulations will be accomplished with a full database of validation study records for both substrates and perpetrators
- We provide extensive literature references, data compilation, slides, and written documentation and GastroPlus model files that can be used for regulatory submissions
- When documentation is in a complete draft form, all components are scientifically reviewed and formatted as a complete package for regulatory review of novel compound results.
- All complete models will be available for download by registered GP license holders.

Acknowledgements

DDI Standards Update Team

Revathi Chapa

Tarang Vora

Georgy Hartman

Joyce Macwan

Naveed Shaik

Grace Fraczkiewicz

Yujuan Zheng

Jin Dong

Saima Subhani

Suvarchala Avvari

Jeremy Perrier

Simulation Technologies Team

Haiying Zhou (TL)

Jim Mullin

Ke Xu Szeto

Jessica Spires

Maxime Le Merdy

Manas Shah

With support from:

Viera Lukacova, Ph.D. (Chief Scientist)

Neil Miller (VP Simulation Sciences)

Andrew Mueller (Project Management)

Arlene Padron (Corp. Marketing Director)

and other teams at Simulations Plus:

Computational Technologies

Consulting Studies

Cheminformatics

Q&A

Questions & Answers

Model-Informed Drug Development

MIDD+

2021 Virtual Conference

For more information about the DDI Standards project email **info@simulations-plus.com**

Register for the 2021 MIDD+ Scientific Conference on March 3rd and 4th. **Bookmark my talk**, on March 3rd at 1:05 PM. **https://www.accelevents.com/e/SLPMIDD**

Learn More! www.simulations-plus.com

SimulationsPlus

Cognigen | DILIsym Services | Lixoft